Published for SISSA by Springer

Received: *July 23, 2025*
Revised: *December 4, 2025*
Accepted: *January 8, 2026*
Published: *March 13, 2026*

Probing the flavour structure of dimension-6 EFT operators in multilepton final states in proton-proton collisions at $\sqrt{s} = 13$ TeV

The CMS collaboration

Full author list at the end of the paper

E-mail: cms-publication-committee-chair@cern.ch

Abstract: An analysis of the flavour structure of dimension-6 effective field theory (EFT) operators in multilepton final states is presented, focusing on the interactions of quarks with Z bosons. For the first time, the flavour structure of these operators is disentangled by simultaneously probing the interactions with different quark generations. The analysis targets the associated production of a top quark pair and a Z boson, as well as diboson processes in final states with at least three leptons, which can be electrons or muons. The data were recorded by the CMS experiment in the years 2016–2018 in proton-proton collisions at a centre-of-mass energy of 13 TeV and correspond to an integrated luminosity of 138 fb^{-1}. Consistency with the standard model of particle physics is observed and limits are set on the selected Wilson coefficients, split into couplings to light- and heavy-quark generations.

Keywords: Flavour Physics, Hadron-Hadron Scattering, Top Physics

ArXiv ePrint: 2507.17498

https://doi.org/10.1007/JHEP03(2026)140

JHEP03(2026)140

Contents

1 Introduction

Despite the known incompleteness of the standard model (SM) of particle physics, no evidence for new physics phenomena has been found in direct searches at the CERN LHC. The reason may lie in the limited energy range of the LHC, which prevents beyond-the-SM (BSM) physics situated at much higher energy scales to be directly produced. However, BSM physics could still leave traces in measurements at the LHC in the form of deviations from the SM prediction. In this case, an effective field theory (EFT) [1–3] is a suitable framework for describing the effects of high-energy BSM phenomena at the energies that can be probed with the LHC. An EFT is valid if the scale of BSM physics, Λ, is well above the energy scale probed by an experiment. The standard model EFT (SMEFT) [2, 4, 5] framework extends the SM Lagrangian with newly introduced operators, organised by their mass dimension. With this, all possible BSM effects are incorporated in an effective Lagrangian, which can be written as

$$\mathcal{L}_{\text{eff}} = \mathcal{L}_{\text{SM}} + \sum_{d,i} \frac{c_i}{\Lambda^{d-4}} \mathcal{O}_i, \tag{1.1}$$

where $\mathcal{L}_{\text{SM}}$ is the Lagrangian of the SM, d is the mass dimension, and $\mathcal{O}_i$ are the newly introduced operators. For each $\mathcal{O}_i$, there exists a dimensionless Wilson coefficient (WC), c_i, scaling the strength of the respective operator. With the SM defined at $d = 4$ and the suppression of the BSM physics with $1/\Lambda^{d-4}$, low mass dimensions, starting at $d = 5$, should become observable first. However, extensions to odd number mass dimensions are assumed

JHEP03(2026)140

to be suppressed as sizeable contributions from these operators lead to the violation of the conservation of lepton or baryon numbers [6]. Thus, in this analysis, only operators of mass dimension $d = 6$ are considered.

A subset of these operators modify the couplings of electroweak (EW) bosons to quarks and can be probed in multiple processes at the LHC. In the top quark sector, these couplings were studied in the context of EFT by the ATLAS [7, 8] and CMS [9–12] Collaborations. Even though many analyses in the CMS programme already probe EFT effects in multiple processes simultaneously [9–12], they only consider the couplings involving top and bottom quarks. However, even in the case of the associated production of a top quark pair ($\mathrm{t\bar{t}}$) and a Z boson ($\mathrm{t\bar{t}Z}$), the Z boson can be radiated from initial-state quarks such that the EW coupling to light-quark generations becomes relevant. In addition, couplings to the light-quark generations enter analyses focusing on top quark processes through background processes such as WZ production in $\mathrm{t\bar{t}Z}$ event selections. In the analysis reported in this article, we probe the flavour structure of dimension-6 EFT couplings by simultaneously measuring the quark couplings with a Z boson for different quark generations. This extends the EFT programme at the LHC by incorporating a greater awareness of flavour dependencies, which are often not considered. We aim to study the interactions between Z bosons and quarks, which are also relevant in neutral-current transitions of b to s quarks of the form $\mathrm{b} \to \mathrm{s}\ell^+\ell^-$ [13, 14], where $\ell^+\ell^-$ denotes a charged-lepton pair. The probed EFT operators are defined in the Warsaw basis [5] and the measurement focuses on those that modify the EW vector couplings,

$$\begin{aligned}
\mathcal{O}_{\varphi q}^{(1)(ab)} &= \left(\varphi^\dagger i\overleftrightarrow{D}_\mu \varphi\right)\left(\overline{q_a}\gamma^\mu q_b\right), \\
\mathcal{O}_{\varphi q}^{(3)(ab)} &= \left(\varphi^\dagger i\overleftrightarrow{D}^I_\mu \varphi\right)\left(\overline{q_a}\gamma^\mu \tau^I q_b\right), \\
\mathcal{O}_{\varphi u}^{(ab)} &= \left(\varphi^\dagger i\overleftrightarrow{D}_\mu \varphi\right)\left(\overline{u_a}\gamma^\mu u_b\right), \text{ and} \\
\mathcal{O}_{\varphi d}^{(ab)} &= \left(\varphi^\dagger i\overleftrightarrow{D}_\mu \varphi\right)\left(\overline{d_a}\gamma^\mu d_b\right),
\end{aligned} \tag{1.2}$$

where φ is the Higgs field, q is the left-handed quark field, u and d are the right-handed quark fields, the indices a and b define the quark flavour, $\overleftrightarrow{D}$ is a two-sided covariant derivative, γ^μ are the gamma matrices, and τ^I are the Pauli sigma matrices. Here, we focus on the diagonal entries of the operators (where $a = b$), such that only processes are considered in which the quark generation remains unchanged after the interaction with an EW boson. Off-diagonal entries would introduce flavour-changing neutral currents, which are tightly constrained and are found to have negligible effect on the selected processes [15–18]. The coupling of the Z boson to quarks is modified by combinations of the respective WCs $c_{\varphi q}^{(1)}$ and $c_{\varphi q}^{(3)}$, while the W boson interaction changes with $c_{\varphi q}^{(3)}$. The right-handed operators $\mathcal{O}_{\varphi u}$ and $\mathcal{O}_{\varphi d}$ are similarly split into the three quark flavours and only modify the coupling to the Z boson. Similar to existing EFT interpretations [9, 12], the probed WCs are reparametrised in the basis of $c_{\varphi q}^{(-)} = c_{\varphi q}^{(1)} - c_{\varphi q}^{(3)}$ and a redefined $c_{\varphi q}^{(3)}$ such that, by adjusting $c_{\varphi q}^{(1)}$ accordingly, $c_{\varphi q}^{(-)}$ remains constant when altering $c_{\varphi q}^{(3)}$. This basis allows a more direct mapping of the operators to the physical couplings of the Z and W bosons.

JHEP03(2026)140

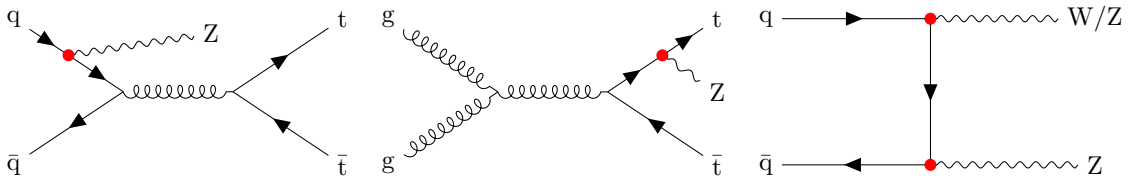

Figure 1. Representative Feynman diagrams showing the leading-order contributions to the $t\bar{t}Z$ production, with the Z boson radiated from the initial-state quarks (left) and from one of the top quarks (middle). The WZ and/or ZZ production is also shown (right). The vertices affected by the EFT operators probed in this analysis are highlighted with red dots.

In order to achieve sensitivity to the flavour structure of the $\mathcal{O}_{\varphi q}^{(1)}$ and $\mathcal{O}_{\varphi q}^{(3)}$ operators, multiple processes with similar multilepton final states are considered. A simultaneous study of $t\bar{t}Z$, WZ, and ZZ production allows us to disentangle the coupling strengths to the third quark generations compared to lighter ones, as shown in figure 1. The $t\bar{t}Z$ process gives sensitivity to the third-generation couplings due to diagrams where the Z boson is radiated from one of the top quarks. In addition, sensitivity to first- and second-generation couplings arises from diagrams where the Z boson is radiated from initial-state quarks. The ZZ and WZ processes increase the constraining power for the first and second quark generations since the bosons are dominantly radiated from light quarks. Since a WWZ vertex can appear in the WZ production process, the operators

$$\begin{aligned} \mathcal{O}_W &= \epsilon^{IJK} W_\mu^{I\nu} W_\nu^{J\rho} W_\rho^{K\mu} \text{ and} \\ \mathcal{O}_{\widetilde{W}} &= \epsilon^{IJK} \widetilde{W}_\mu^{I\nu} W_\nu^{J\rho} W_\rho^{K\mu}, \end{aligned} \tag{1.3}$$

where W is the W boson field and ϵ is the Levi-Civita symbol, are considered in this analysis as well. We always target the leptonic decay of the Z boson and select final states containing three or four electrons and muons, referred to simply as leptons from hereon. This choice ensures a high-quality reconstruction of the Z boson, which is our handle to provide a highly pure sample of signal processes. A profiled likelihood fit to the distribution in the transverse momentum, p_{T}, of the reconstructed Z boson candidate is used to probe the EFT effects. The fit is performed simultaneously in three signal regions (SRs) that target the $t\bar{t}Z$, WZ, and ZZ processes. Control regions (CRs) are defined to estimate the background contribution from processes with nonprompt leptons.

In this analysis, proton-proton (pp) collision data are used, collected at $\sqrt{s} = 13\,\mathrm{TeV}$ in 2016–2018 and corresponding to an integrated luminosity of $138\,\mathrm{fb}^{-1}$. Dimension-6 EFT operators and the corresponding WCs $c_{\varphi q}^{(-)}$, $c_{\varphi q}^{(3)}$, $c_{\varphi u}$, $c_{\varphi d}$, c_W, and $c_{\widetilde{W}}$ are probed. Aiming towards a more global interpretation, the flavour-dependent interaction strengths of the aforementioned EFT operators are simultaneously targeted in $t\bar{t}Z$, WZ, and ZZ processes, accounting for correlations of EFT effects in these processes by construction. Moreover, this approach enables a proper and consistent treatment of the correlations between systematic uncertainties, which is crucial for ensuring the reliability of the interpretations of the results. Other operators such as $\mathcal{O}_{tZ}$ and $\mathcal{O}_{tW}$ are not considered as they are already strongly constrained in other analyses of $t\bar{t}$ production in association with a Z boson [7, 9–12]. In

JHEP03(2026)140

addition, measurements including the associated production of a $t\bar{t}$ pair with a photon ($t\bar{t}\gamma$) [8, 19] provide even more stringent limits.

The paper is organised as follows. The CMS detector is described in section 2 and the simulated event samples are detailed in section 3. Sections 4 and 5 discuss the reconstruction of physics objects and the event selection in the various regions of the analysis, respectively. The background estimation of processes with nonprompt leptons is detailed in section 6. In section 7, we explain sources of systematic uncertainties and their estimation. The profiled maximum likelihood fit to data and results are discussed in section 8 and, lastly, a summary is provided in section 9. Tabulated results are provided in the HEPData record for this analysis [20].

2 The CMS detector

The central feature of the CMS detector is a superconducting solenoid of 6 m internal diameter, providing a magnetic field of 3.8 T. A silicon pixel and strip tracker, a lead tungstate crystal electromagnetic calorimeter (ECAL), and a brass and scintillator hadron calorimeter (HCAL), each composed of a central barrel and two endcap sections, reside within the solenoid volume. Forward calorimeters extend the pseudorapidity (η) coverage provided by the barrel and endcap detectors. Muons are detected in gas-ionisation chambers embedded in the steel flux-return yoke outside the solenoid. A more detailed description of the CMS detector, together with a definition of the coordinate system, can be found in ref. [21]. Between the 2016 and 2017 data-taking runs, the CMS pixel detector was upgraded with additional layers in the barrel and endcap regions of the CMS detector. Details about the changes can be found in ref. [22].

Events of interest are selected using a two-tiered trigger system. The first level, composed of custom hardware processors, uses information from the calorimeters and muon detectors to select events at a rate of around 100 kHz within a fixed latency of about 4 μs [23]. The second level, known as the high-level trigger, consists of a farm of processors running a version of the full event reconstruction software optimised for fast processing, and reduces the event rate to a few kHz before data storage [24, 25].

3 Simulated event samples

We simulate all processes that are compatible with our selected final state and apply the same reconstruction and event selection as for data. The standard model predictions of the $t\bar{t}Z$, WZ, and ZZ processes are obtained by simulating events at next-to-leading order (NLO) in perturbative quantum chromodynamics (QCD). We use MadGraph5_aMC@NLO v2.6.5 [26, 27] for $t\bar{t}Z$ production and POWHEG v2 [28, 29] for WZ and ZZ. For the prediction of EFT effects, alternative samples of the $t\bar{t}Z$, WZ, and ZZ processes are simulated using MadGraph5_aMC@NLO at leading order (LO) in QCD and in EW theory with up to one additional parton simulated in the matrix element calculations. A reweighting method [30] is used to reproduce the effect of different WC values on event distributions. The total matrix elements are calculated at several points in the EFT parameter space using the

JHEP03(2026)140

SMEFTsim package [31, 32] via

$$|\mathcal{M}|^2 = |\mathcal{M}_{\text{SM}}|^2 + \sum_i 2c_i \text{Re}(\mathcal{M}^*_{\text{SM}}\mathcal{M}^i_{\text{BSM}}) + \sum_i \sum_j c_i c_j \text{Re}(\mathcal{M}^{*i}_{\text{BSM}}\mathcal{M}^j_{\text{BSM}}), \tag{3.1}$$

where $\mathcal{M}_{\text{SM}}$ and $\mathcal{M}_{\text{BSM}}$ are the matrix element contributions from SM and BSM physics, respectively. The WCs, c_i, are assumed to be real and the sum runs over all considered EFT operators. Weights corresponding to the ratios $|\mathcal{M}|^2/|\mathcal{M}_{\text{SM}}|^2$ for selected base points in the EFT parameter space are stored for each simulated event. With $(N+1)(N+2)/2$ of these weights, the polynomial for N EFT operators is solved to extract weights, containing the full dependence on WCs, on an event-by-event basis. In the computation of $\mathcal{M}$, we only consider diagrams with a single EFT vertex such that terms linear in c encode the SM-BSM interference and quadratic terms describe the pure BSM contribution. Setting all WCs to zero, the LO samples with an additional parton are verified to reproduce — within renormalisation and factorisation scale uncertainties estimated following the description in section 7 — the SM distributions modelled at NLO in perturbative QCD. The predictions at NLO are used for the SM scenario of $\text{t}\bar{\text{t}}\text{Z}$, WZ, and ZZ and samples with EFT weights are only used to predict the EFT effects.

Top quark pair production, $\text{t}\bar{\text{t}}$ production in association with a Higgs boson ($\text{t}\bar{\text{t}}\text{H}$), and single top t-channel and tW processes are simulated at NLO in QCD using POWHEG [33–39]. The MadGraph5_aMC@NLO generator is used for the simulation of $\text{t}\bar{\text{t}}\text{W}$, $\text{t}\bar{\text{t}}\text{t}\bar{\text{t}}$, tWZ, tZq, and triboson production (WWW, WWZ, WZZ, and ZZZ) at NLO in QCD. The Drell-Yan process, W+jets, and $\text{t}\bar{\text{t}}$ production in association with two bosons ($\text{t}\bar{\text{t}}\text{WW}$, $\text{t}\bar{\text{t}}\text{WZ}$, $\text{t}\bar{\text{t}}\text{ZZ}$) are simulated with MadGraph5_aMC@NLO at LO. In the following, we group the $\text{t}\bar{\text{t}}\text{W}$, $\text{t}\bar{\text{t}}\text{H}$, $\text{t}\bar{\text{t}}\text{WW}$, $\text{t}\bar{\text{t}}\text{WZ}$, $\text{t}\bar{\text{t}}\text{ZZ}$, and $\text{t}\bar{\text{t}}\text{t}\bar{\text{t}}$ processes as $\text{t}\bar{\text{t}}\text{X}$.

The WW process and gluon-initiated ZZ production ($\text{gg} \to \text{ZZ}$) are simulated at LO with PYTHIA 8.240 [40] and the MCFM v7.0.1 generator [41–43], respectively. Other processes, such as the production of $\text{t}\bar{\text{t}}\gamma$, the simultaneous production of a Z boson and a photon, additional processes with a Higgs boson decaying to a pair of Z bosons, and the purely EW production of $\text{t}\bar{\text{t}}\text{W}$ were found to contribute to less than 1% to all the selected events and are therefore neglected.

For all processes, the parton shower, multiple parton interactions, and hadronization is simulated using PYTHIA 8.230 with the CP5 tune [44]. The matrix element calculation and parton shower simulation are matched using the FxFx [45] and MLM [46] algorithms for the processes simulated with MadGraph5_aMC@NLO at NLO and LO, respectively. All simulated samples use the NNPDF3.1 [47] parton distribution functions (PDFs) at next-to-NLO accuracy.

The interaction of particles with and response of the detector are simulated with the Geant4 package [48, 49]. In addition, pp inelastic collisions simulated with PYTHIA are mixed into each event to model the effect from additional collisions within the same or adjacent bunch crossing (pileup).

4 Event reconstruction

The particle-flow (PF) algorithm [50] aims to reconstruct and identify each individual particle in an event, using an optimised combination of information from the various elements of

JHEP03(2026)140

the CMS detector. The primary vertex is taken to be the vertex corresponding to the hardest scattering in the event, evaluated using tracking information alone, as described in section 9.4.1 of ref. [51]. The missing transverse momentum vector $\vec{p}_{\mathrm{T}}^{\,\mathrm{miss}}$ is computed as the negative vector sum of the transverse momenta of all the PF candidates in an event, and its magnitude is denoted as $p_{\mathrm{T}}^{\mathrm{miss}}$ [52]. The $\vec{p}_{\mathrm{T}}^{\,\mathrm{miss}}$ is modified to account for corrections to the energy scale of the reconstructed jets in the event.

The energy of photons is obtained from the ECAL measurement [53]. The energy of electrons is determined from a combination of the track momentum at the main interaction vertex, the corresponding ECAL cluster energy, and the energy sum of all bremsstrahlung photons attached to the track. Muons are reconstructed from tracks in the inner tracker that extend to the muon system. From the curvature of the track, their momentum can be precisely determined [54]. Both muons and electrons must pass tight quality criteria developed by the CMS Collaboration to ensure a proper reconstruction [53, 54].

The energy of charged hadrons is determined from a combination of the track momentum and the corresponding ECAL and HCAL energy deposits, corrected for the response function of the calorimeters to hadronic showers. Finally, the energy of neutral hadrons is obtained from energy measurements in ECAL and HCAL [50].

Electrons are further required to have $p_{\mathrm{T}} > 10\,\mathrm{GeV}$ and $|\eta| < 2.5$, excluding $1.44 < |\eta| < 1.57$ that corresponds to the ECAL transition region. Muons are selected with $|\eta| < 2.4$ and the same p_{T} requirement as that for the electrons. In order to be considered for the analysis, electrons and muons must pass additional quality criteria [53, 54], that concern the number of reconstructed hits in the tracker and/or muon system, their compatibility with originating from the primary vertex, the quality of charge reconstruction, and isolation from other activities in the detector. In addition, we make use of a multivariate analysis that is trained to distinguish prompt leptons from those that originate from heavy-flavour hadron decays and/or misidentified jets [55, 56], referred to as nonprompt leptons. Following the definition in ref. [55], two identification working points (WPs), 'loose' and 'tight', are used. Tight leptons are used in the selection of events in the signal region, while the estimation of nonprompt backgrounds is based on a selection of leptons passing the loose but failing the tight WP in dedicated control regions in data. The efficiency and misidentification rate for selecting tight muons with $p_{\mathrm{T}} > 25\,\mathrm{GeV}$ ($10 < p_{\mathrm{T}} < 25\,\mathrm{GeV}$) were estimated in $\mathrm{t\bar{t}}$ simulation to be 96 (75)% and 1 (0.9)% [55], respectively. For electrons with $p_{\mathrm{T}} > 25\,\mathrm{GeV}$ ($10 < p_{\mathrm{T}} < 25\,\mathrm{GeV}$), the selected WP corresponds to a selection efficiency and misidentification rate of 93 (64)% and 0.6 (0.4)% [55].

For each event, hadronic jets are clustered from these reconstructed PF particles using the infrared and collinear safe anti-k_{T} algorithm [57, 58] with a distance parameter of 0.4. Jet momentum is determined as the vectorial sum of all particle momenta in the jet, and is found from simulation to be, on average, within 5 to 10% of the true momentum over the whole p_{T} spectrum and detector acceptance. For jets to be considered in this analysis, they are required to have $p_{\mathrm{T}} > 30\,\mathrm{GeV}$ and be within $|\eta| < 2.4$. Pileup can contribute additional tracks and calorimetric energy depositions to the jet momentum. To mitigate this effect, charged particles identified to be originating from pileup vertices are discarded and an offset correction is applied to correct for remaining contributions. Jet energy corrections [59] are

JHEP03(2026)140

derived from simulation to bring the measured response of jets to that of particle level jets on average. The energy scale corrections are propagated to $p_{\mathrm{T}}^{\mathrm{miss}}$.

Jets initiated by the hadronization of b quarks (b jets) are identified using the DeepJet algorithm [60, 61]. The WP chosen for this analysis corresponds to a misidentification rate of 0.1% for light-flavour quark and gluon jets, and an efficiency of 68% for b jets.

5 Event selection

The data for this analysis are selected using a combination of electron and muon triggers. With respect to the baseline selection detailed below, we obtain a trigger efficiency of more than 99%, using a combination of triggers that require single or multiple leptons with p_{T} thresholds between 5 and 40 GeV. Further selection criteria are defined offline in order to select regions that contain a mostly pure sample of the target processes $\mathrm{t\bar{t}Z}$, WZ, and ZZ. For each process, a dedicated SR is defined, resulting in three regions $\mathrm{SR}_{\mathrm{t\bar{t}Z}}$, $\mathrm{SR}_{\mathrm{WZ}}$, and $\mathrm{SR}_{\mathrm{ZZ}}$. The nonprompt lepton contributions in $\mathrm{SR}_{\mathrm{t\bar{t}Z}}$ and $\mathrm{SR}_{\mathrm{WZ}}$ are derived from CRs that are labelled $\mathrm{CR}_{\mathrm{t\bar{t}Z}}$ and $\mathrm{CR}_{\mathrm{WZ}}$. In $\mathrm{SR}_{\mathrm{ZZ}}$, the contribution from nonprompt leptons is negligible and no corresponding CR is introduced.

All SRs and CRs are based on a common baseline selection. This baseline selection requires at least three leptons (electrons or muons) that pass the loose WP, with $p_{\mathrm{T}} > 40$, 20, and 10 GeV. We do not explicitly veto electrons or muons from leptonic tau lepton decays. To remove leptonic decays of low-mass resonances, events are selected where all pairwise combinations of leptons have an invariant mass above 12 GeV. Furthermore, at least one lepton pair of same flavour and opposite electric charge is required to have an invariant mass compatible with the Z boson mass of 91 GeV [62] ($81 < m_{\ell\ell} < 101$ GeV). If multiple pairs satisfy these criteria, the pair closest to the Z boson mass is considered a Z boson candidate. For events with four leptons, a second Z boson candidate, with similar requirements, is constructed from the remaining two leptons after the pair of leptons closest to the Z boson mass is removed from the list.

The signal region $\mathrm{SR}_{\mathrm{t\bar{t}Z}}$ additionally requires events to contain exactly three tight leptons without additional loose leptons. A large fraction of nonprompt leptons are rejected as a result of this selection and the remaining ones are estimated from data. To reduce the WZ contribution, at least one jet must be b tagged. The contribution of tZq production is reduced by requiring at least three jets. From simulation, we expect the yield to be about 60% $\mathrm{t\bar{t}Z}$ events with a subleading contribution of up to 10% from WZ production. In $\mathrm{SR}_{\mathrm{WZ}}$, events are required to pass the baseline selection and to contain exactly three leptons passing the tight WP. Events with additional loose leptons are vetoed. To enhance leptonic decays of the W boson, events with $p_{\mathrm{T}}^{\mathrm{miss}} > 60$ GeV are selected. In order to construct a region orthogonal to $\mathrm{SR}_{\mathrm{t\bar{t}Z}}$ and suppress processes with top quarks, events without any b-tagged jets are selected. In $\mathrm{SR}_{\mathrm{WZ}}$, 87% of the events originate from WZ production. The region $\mathrm{SR}_{\mathrm{ZZ}}$ is defined by the baseline selection, requiring four leptons with tight identification criteria. Events must contain two Z boson candidates following the requirements detailed earlier. The region is very pure in ZZ production (99%) and has a negligible background contribution. The effects of the EFT operators probed in this analysis are displayed in each of the SRs in figure 2, where the target process in each of the three SRs is shown at the SM point and

JHEP03(2026)140

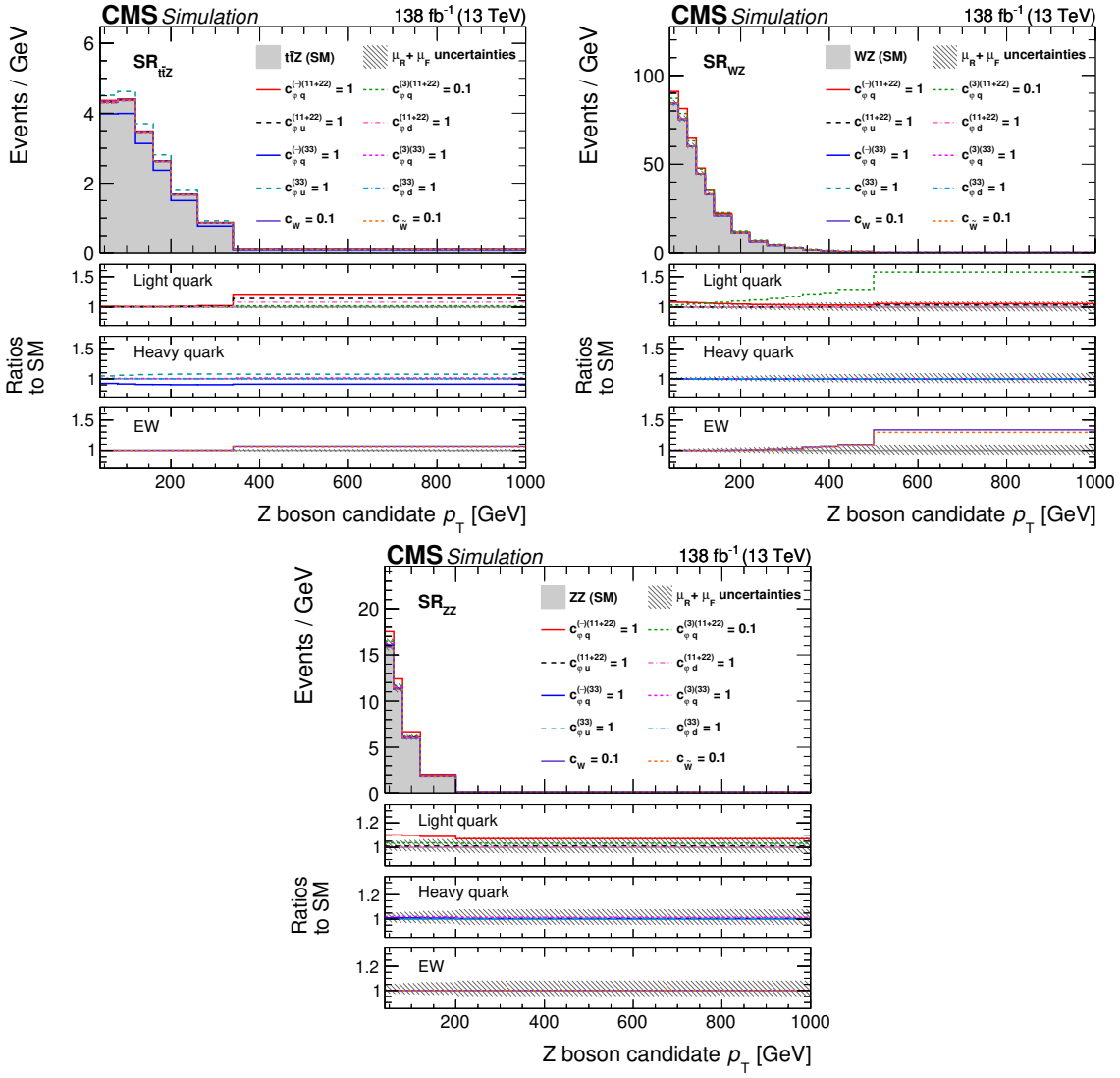

Figure 2. Distributions of the Z boson p_T in the three signal regions of this analysis. Shown are $SR_{t\bar{t}Z}$ (upper left), SR_{WZ} (upper right), and SR_{ZZ} (lower). In each region, the target process ($t\bar{t}Z$, WZ, or ZZ) is shown at the SM point (coloured areas) and various EFT hypotheses (lines). The hashed band includes only uncertainties in the renormalisation and factorisation scales (μ_R and μ_F). The upper, middle, and lower ratio panels show the ratio of EFT hypotheses for light-quark, heavy-quark, and EW boson couplings, respectively. The bin content is divided by the bin width.

compared to selected EFT hypotheses. It is clearly visible that the $t\bar{t}Z$ process is sensitive to the third-generation couplings, while WZ and ZZ can constrain the couplings of light quarks to EW bosons. Furthermore, the $t\bar{t}Z$ process adds to the sensitivity of the first and second generations since the Z boson can be radiated from initial-state light quarks. The radiation from initial-state quarks is enhanced at large Z boson p_T, which increases the sensitivity to light-quark couplings and reduces it for heavy-quark couplings in the $t\bar{t}Z$ process at high p_T.

The control regions $CR_{t\bar{t}Z}$ and CR_{WZ} have the same criteria as the corresponding SRs with the exception that at least one of the selected leptons must fail the tight WP of the

JHEP03(2026)140

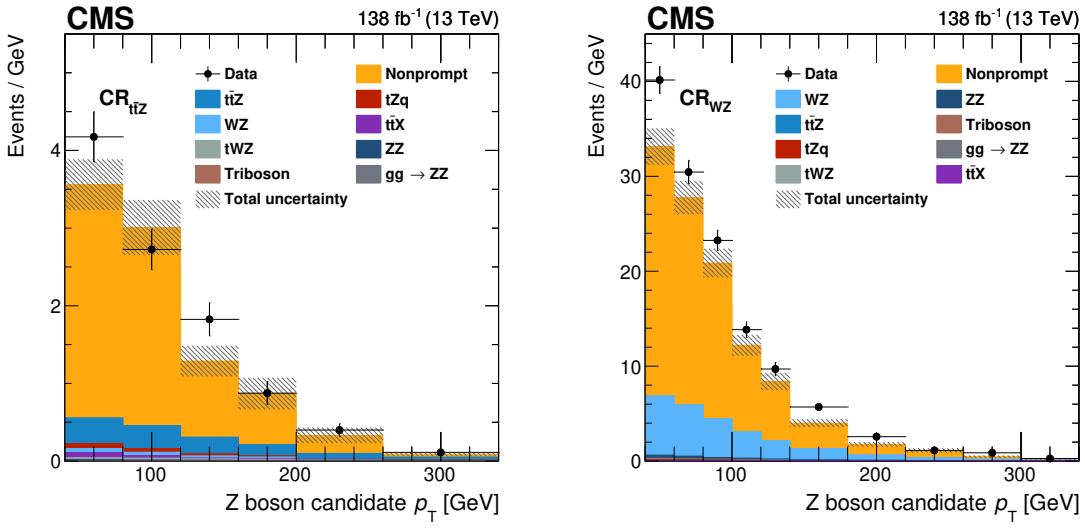

Figure 3. Distributions of the Z boson p_T in the control regions of this analysis. Shown are $CR_{t\bar{t}Z}$ (left) and CR_{WZ} (right). Predictions are all obtained from simulation and are displayed as coloured areas. The hashed area shows the statistical uncertainty in the prediction. Data are displayed as markers, where the vertical bars represent the statistical uncertainty. The bin content is divided by the bin width.

lepton identification. Figure 3 shows the Z boson p_T distributions in the two CRs for data and simulation. They are enriched in contributions from nonprompt leptons and allow the estimation of the nonprompt contribution in the signal regions $SR_{t\bar{t}Z}$ and SR_{WZ} as further discussed in the following section. The nonprompt contribution shown for illustration in figure 3 is obtained from simulated events.

6 Background estimation

The processes targeted in this analysis are rare in comparison with other processes involving final-state leptons at the LHC. Thus, despite large lepton identification efficiencies and small misidentification rates, processes with nonprompt leptons significantly contribute to the selected SRs. The origin of nonprompt leptons is manifold. In the SRs of this analysis, nonprompt leptons mostly occur in Drell-Yan or $t\bar{t}$ production, where the third lepton is nonprompt. We distinguish nonprompt electrons, which tend to be misidentified jets in Drell-Yan processes, and nonprompt muons, which mostly originate from heavy-flavour decays in the parton shower, e.g. in $t\bar{t}$ events.

Since nonprompt leptons are difficult to model in simulation, their contribution is estimated from data [12, 55, 63, 64] by using $CR_{t\bar{t}Z}$ and CR_{WZ}. To estimate the contribution in the SRs, a transfer factor, w, is applied to the nonprompt contribution measured in the CRs. It is a function of the misidentification rate, i.e. the probability that a nonprompt lepton that passes the loose identification also passes the tight WP. The transfer factor is

$$w = (-1)^{N_\ell - 1} \prod_i^{N_\ell} \frac{f_i}{1 - f_i}, \tag{6.1}$$

JHEP03(2026)140

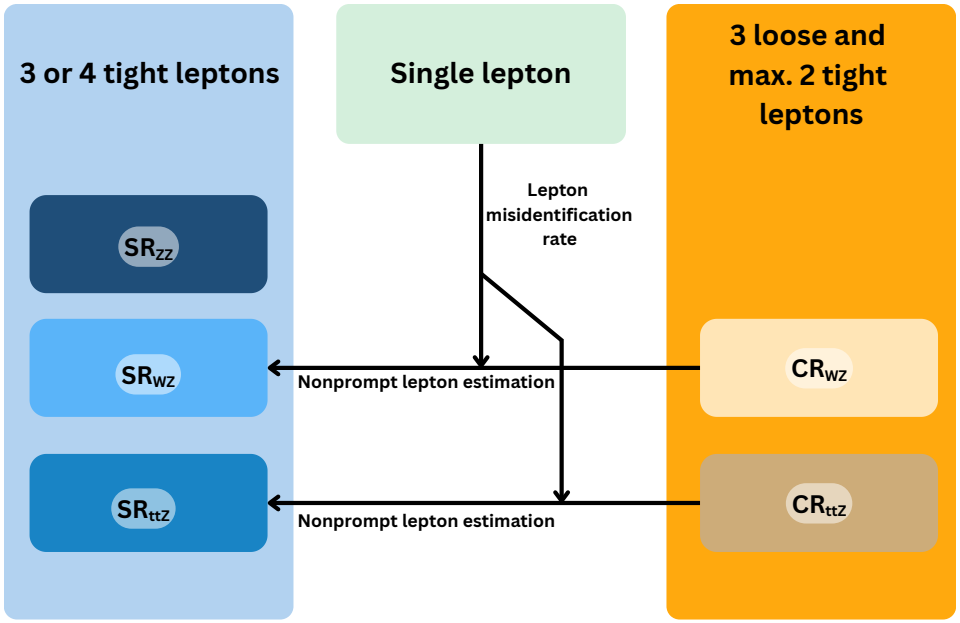

Figure 4. Schematic representation of the SRs and CRs used in this analysis. The application of the estimated nonprompt lepton background from the CRs into the SRs is illustrated with arrows.

where f_i is the misidentification rate of the i-th lepton that does not fulfil the tight identification and N_ℓ is the total number of leptons that fail the tight identification. The sign flip eliminates double counting [63] of the probability in events where multiple leptons do not pass the tight identification.

The misidentification rate f is measured in additional single-lepton CRs. In these CRs, events are selected with single electron or single muon triggers with muon (electron) p_{T} thresholds as low as 3 (8) GeV; we require that events have exactly one lepton with $p_{\mathrm{T}} > 10\,\mathrm{GeV}$ and $|\eta| < 2.4$ (2.5) that passes the loose WP, at least one jet with an angular separation $\Delta R > 0.7$ from the lepton, and $p_{\mathrm{T}}^{\mathrm{miss}} < 20\,\mathrm{GeV}$. The selection criteria are chosen such that a rich sample of nonprompt leptons is selected. The misidentification rate f is measured in data after subtracting the prompt contribution estimated from simulation and differentially in lepton flavour (electrons and muons), p_{T}, η, and year of data taking. It has values between 0.15 and 0.8. A schematic representation of all SRs and CRs is displayed in figure 4, together with the strategy for estimating the nonprompt lepton background in the SRs.

In addition to the statistical uncertainty in the measurement of the misidentification rates, a modelling uncertainty is assigned to account for potential nonclosure, which is estimated in data and simulation. In data, the background estimation is tested in validation regions (VRs) orthogonal to $\mathrm{SR}_{\mathrm{t\bar{t}Z}}$ and $\mathrm{SR}_{\mathrm{WZ}}$, where all selection criteria remain, but no Z boson candidate in the mass range 81–101 GeV can be formed from two opposite-sign leptons of same flavour ($\mathrm{VR}_{\mathrm{t\bar{t}Z}}$) or the missing transverse momentum is below 60 GeV ($\mathrm{VR}_{\mathrm{WZ}}$). In the VRs, the contribution of nonprompt leptons is enhanced with respect to the SRs, and the data agree with the estimated event yields after a fit that only includes the uncertainties related

JHEP03(2026)140

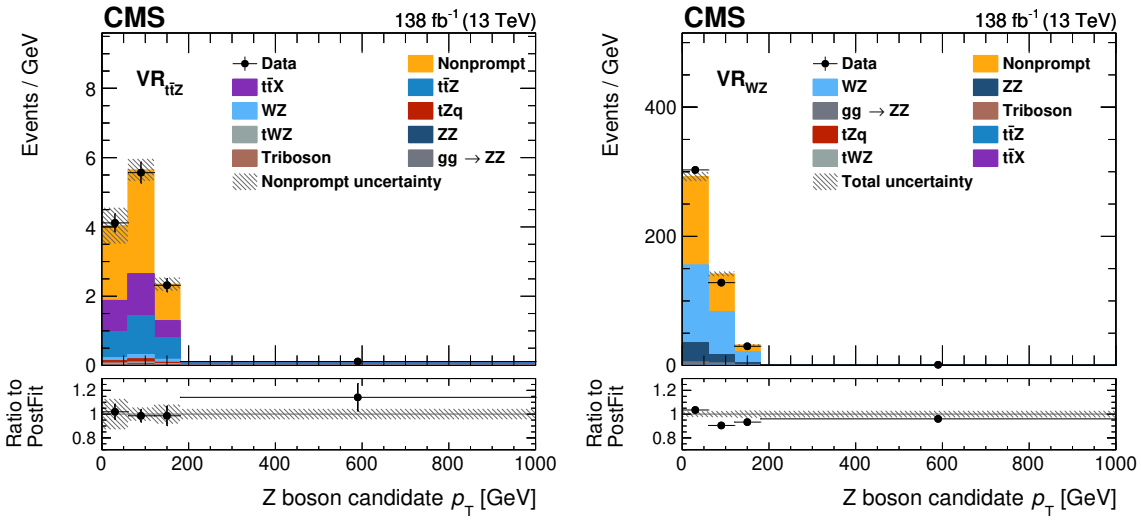

Figure 5. Distributions of the Z boson p_T in the two validation regions $VR_{t\bar{t}Z}$ (left) and VR_{WZ} (right) after a fit including only uncertainties in the nonprompt lepton estimation. The data (markers) are compared to the prediction from simulation and the data-driven estimate of nonprompt leptons (coloured areas). The lower panel displays the ratio to the predictions after the fit. The hashed area displays the uncertainties in the estimation of the nonprompt lepton background after the fit. The bin content is divided by the bin width.

to the background estimation, as shown in figure 5. For the estimation of the nonprompt lepton contribution in the VRs, dedicated CRs are constructed analogously to those used for the estimation in the SRs. Along with the Z candidate p_T, other observables such as the p_T distributions of the three selected leptons were tested as well. In addition to the test in data, we fit the estimated contribution of nonprompt leptons to the true contribution in simulation and verify that the uncertainty model is flexible enough to fit a residual nonclosure.

In total, the nonclosure uncertainty consists of 15 components, divided into three lepton flavour categories and five correlation patterns. For the flavour categories, we identify if only muons, only electrons, or a mixture of both do not satisfy the tight lepton identification criteria. The correlation patterns assign each of the data-taking periods an uncorrelated part and one that correlates the uncertainty between all periods. Each uncertainty amounts to a normalisation uncertainty of 25%. We observe closure in all tests when considering only the uncertainties corresponding to the nonprompt-lepton background estimation.

Contributions from photon conversions through interactions with the detector material are drastically reduced by the lepton identification criteria. Studies with simulated $t\bar{t}\gamma$ events showed that this contribution is negligible in all regions of the analysis.

All processes with prompt leptons — $t\bar{t}Z$, WZ, ZZ, tZq, tWZ, $t\bar{t}X$, or the production of three EW bosons — are estimated from simulation, as described in section 3.

7 Systematic uncertainties

Systematic uncertainties are split into experimental and theory components, depending on their origin. Each uncertainty is implemented as one or multiple nuisance parameters in the

JHEP03(2026)140

profiled likelihood fit and is evaluated for both the SM and the EFT predictions. For most extracted WCs, the uncertainties in the production cross section of the $t\bar{t}Z$, WZ, and ZZ processes have the largest impact among the systematic uncertainties.

7.1 Experimental uncertainties

Experimental uncertainties arise from the calibration of physics objects that are used in the analysis, from efficiency corrections in the simulation, and from the estimation of background processes. The uncertainties are implemented in this analysis by propagating shifts of ± 1 standard deviations to the distributions used in the fit.

The uncertainty in the lepton identification [53, 54] efficiency is measured as a function of the lepton flavour, p_T, and η. Based on whether the uncertainties have statistical or systematic origin, they are split into uncorrelated and correlated parts for the four data-taking periods, since the year 2016 is split into two periods. This uncertainty is modelled with a total of 10 nuisance parameters in the profiled likelihood fit discussed below. An additional parameter models the uncertainty in the electron reconstruction efficiency, which is treated as correlated for data-taking periods.

The uncertainty in the correction of the b tagging [65] efficiency is a function of jet p_T, η, b tagging WP, as well as flavour. The uncertainty is split in correlated and uncorrelated parts across the data-taking periods and is modelled with 10 nuisance parameters.

The pileup profile in the simulation is weighted to match the pileup profile observed in data [66]. Observables sensitive to pileup are used to estimate the effective value for the inelastic pp cross section of $69.2\,\text{mb} \pm 4.6\%$, where the uncertainty accounts for remaining differences between data and simulation. In this analysis, the event weight is varied within this uncertainty. The uncertainty is modelled with a single parameter.

The efficiency of the combination of triggers [24] used in this analysis is measured using a sample of events collected with an independent trigger to be larger than 99% in the selected phase space for data and simulation. We do not assign any correction of the trigger efficiency in simulation but consider a 1% uncertainty that represents the statistical uncertainty in the efficiency measurement in data for each data-taking period, resulting in four nuisance parameters. A gradual shift in the timing of the ECAL and muon systems causes inefficiencies of the first-level trigger system that is not included in the simulation [23] and not accounted for by the aforementioned efficiency measurements. With auxiliary measurements of these inefficiencies in data, the effect is modelled in simulation. A corresponding systematic uncertainty is modelled with a single nuisance parameter.

In the estimation of the nonprompt background, the precision of the measured misidentification rate is limited by the number of selected events in the single lepton CRs where the lepton misidentification rate is measured. This statistical uncertainty is split by lepton flavour and data-taking period and propagated to the estimation of the nonprompt background in the SRs. In addition, various normalisation uncertainties are assigned to cover the potential nonclosure of this method. We split into an uncorrelated and a correlated part across the data-taking periods as well as split the uncertainty according to the misidentified-lepton flavour. As detailed in section 6, this leads to a total of 15 nuisance parameters.

JHEP03(2026)140

The integrated luminosity is measured with a precision of 1.2, 2.3, and 2.5% in the data-taking periods of 2016, 2017, and 2018 [67–69]. The luminosity uncertainties are partly correlated between the three years. This results in uncorrelated uncertainties of 1.0, 2.0, and 1.5% for the three years. A correlated part among all data-taking years contributes as 0.6, 0.9, and 2.0% for 2016, 2017, and 2018. Lastly, correlations between 2017 and 2018 amount to uncertainties of 0.6 and 0.2%. This results in a total of five nuisance parameters.

The jet four-momenta are varied within the uncertainties in the jet energy scale, considering various uncertainty sources split between detector regions and data-taking periods [59]. Also, the jet four-momenta are varied within the uncertainties in the jet energy resolution smearing. This uncertainty is considered uncorrelated for all data-taking periods such that four nuisance parameters are introduced. All these variations are also propagated to $p_{\mathrm{T}}^{\mathrm{miss}}$.

The missing transverse momentum is corrected for PF candidates that are not clustered into jets. We vary $p_{\mathrm{T}}^{\mathrm{miss}}$ within the corresponding uncertainty using four parameters for uncorrelated effects between data-taking periods.

7.2 Theory uncertainties

Various uncertainties are associated with our limited knowledge in the modelling of all simulated processes relevant to this analysis. This includes uncertainties that only affect the normalisation and those that change the shape and acceptance.

The factorisation and renormalisation scales are varied independently by factors of 0.5 and 2 and we construct nuisance parameters for each process. Here, only differences in the shape and acceptance of the distributions and not in the normalisation are considered. In order to test the assumption of uncorrelated uncertainties, the impact of correlations was studied in the WZ and ZZ processes by performing the profiled likelihood fit with fully correlated and uncorrelated setups. The differences in the resulting likelihoods was found to be negligible. Thus, per process, one nuisance parameter is introduced to model the uncertainty in the factorisation scale and another parameter for the renormalisation scales, which amount to a total of 14 parameters in the likelihood fit.

Uncertainties in the proton PDFs are estimated by using NNPDF replicas [47, 70], resulting in 100 variations. For each variation a nuisance parameter is constructed in the fit, correlating all processes. Similar to scale variations, only shape and acceptance effects from the event selection are considered. Normalisation effects are absorbed into uncertainties in the production cross section described below.

Parton shower uncertainties are estimated by varying the energy scales of the initial-state radiation (ISR) and final-state radiation (FSR) individually by factors of 0.5 and 2. Similar to scale variations, only shape and acceptance effects are considered. The ISR uncertainties are split into nuisance parameters for each process, whereas the FSR uncertainty is correlated between processes. This results in a total of eight nuisance parameters for parton shower uncertainties.

We consider production-rate uncertainties arising from the limited accuracy of the computed process cross sections, uncertainties in dedicated measurements, and the small number of simulated events that pass the analysis selection. These uncertainties only affect the normalisation of a process and are correlated among all years. A 20% uncertainty is assigned

JHEP03(2026)140

to tWZ, triboson production, as well as $t\bar{t}X$ processes, which include $t\bar{t}W$ [71], $t\bar{t}H$ [72], $t\bar{t}WW$, $t\bar{t}WZ$, $t\bar{t}ZZ$, and $t\bar{t}t\bar{t}$. Although recent measurements of the inclusive $t\bar{t}W$ cross section showed a much larger value compared to the SM prediction, the $t\bar{t}W$ contribution in this analysis is so small that enhancing the corresponding cross section or its uncertainty does not alter the results. We assign uncertainties of 10 [73] and 11% [72] to the production cross sections of the tZq and $t\bar{t}Z$ processes, respectively. The diboson processes WZ and ZZ are assigned rate uncertainties of 5% [74, 75]. This results in a total of seven nuisance parameters. For the tZq and tWZ production, additional 20% rate uncertainties are assigned accounting for the missing EFT effects in the simulations of these processes, estimated from the EFT effects observed in ref. [11]. Since those processes only contribute a small amount in our selected phase space, this uncertainty has a negligible effect on the extracted WCs.

The modelling of the number of associated jets in WZ production in a similar phase space was found to be not well described in the observation of the $t\bar{t}t\bar{t}$ production [55]. The correction factor is applied as a function of the number of jets and reaches from 0.85 for one jet to 2.69 for six jets. The difference between not applying and applying the correction factors measured in ref. [55] is used as an uncertainty, which is implemented as a single nuisance parameter. However, the correlation with the sensitive observable used in this analysis, the reconstructed Z boson p_{T}, is small such that this uncertainty is only relevant in $\mathrm{SR}_{t\bar{t}Z}$, where three jets are required. Here the uncertainty only impacts the total WZ event yield by about 20% in $\mathrm{SR}_{t\bar{t}Z}$. With a signal injection test it is ensured that a varied modelling of jet multiplicity in WZ production does not bias the extraction of EFT effects.

In order to estimate the uncertainty in the modelling of WZ plus heavy-flavour quarks, an additional 20% normalisation uncertainty is assigned for simulated WZ events that are produced in association with c and b quarks [73]. Also this uncertainty is modelled with a single parameter in the fit.

For the processes WZ and ZZ we assign an uncertainty corresponding to the estimated EW corrections to the production cross section obtained in ref. [76]. The uncertainty is implemented as a function of the true Z boson p_{T} in simulation. Four nuisance parameters are implemented to model the additive and multiplicative corrections to WZ and ZZ production.

8 Maximum likelihood fit and results

We extract the values of the WCs in a maximum likelihood fit to data, using the CMS statistical analysis tool Combine [77], based on the RooFit [78] and RooStats [79] frameworks. In this setup, the WCs are the parameters of interest, and we estimate the effects of terms in the matrix element that depend linearly and quadratically on the WCs. We simultaneously fit the Z boson p_{T} distributions in the regions $\mathrm{SR}_{t\bar{t}Z}$, $\mathrm{SR}_{\mathrm{WZ}}$, and $\mathrm{SR}_{\mathrm{ZZ}}$, allowing for sensitivity to all operators, while other observables — such as angular distances between leptons or Z boson candidates — do not result in a more sensitive probe. The likelihood is built from Poisson probabilities to observe the per-bin event yields in data given the signal and background predictions. Sources of systematic uncertainties are modelled with nuisance parameters in the fit. Shape uncertainties are implemented using a Gaussian distribution and rate uncertainties are modelled with a log-normal distribution. Statistical uncertainties related to the finite number of simulated events are modelled with a single

JHEP03(2026)140

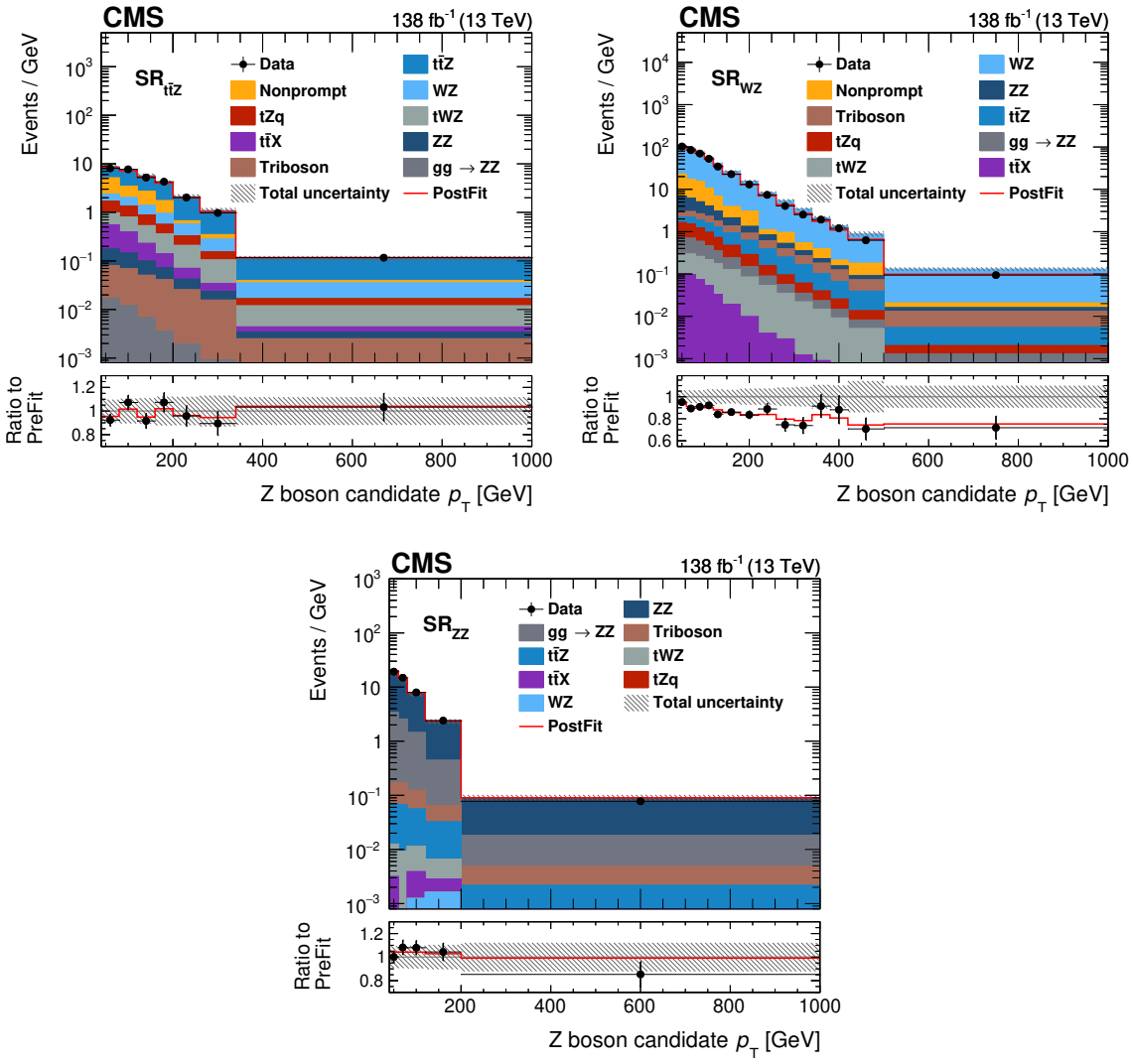

Figure 6. Distributions of the Z boson p_{T} in the three signal regions of this analysis. Shown are the $\mathrm{SR}_{\mathrm{t\bar{t}Z}}$ (upper left), $\mathrm{SR}_{\mathrm{WZ}}$ (upper right), and $\mathrm{SR}_{\mathrm{ZZ}}$ (lower) regions. The data (markers) are compared to the prediction from simulation and the data-driven estimate of nonprompt leptons (coloured areas). The lower panel displays the ratio to the predictions before the fit. The hashed area displays the total uncertainties before the likelihood fit and the red line displays the best fit result in a setup with all EFT parameters. The bin content is divided by the bin width.

nuisance parameter per bin in the fit (Barlow-Beeston lite) [80]. Figure 6 shows the fitted distributions, including the best fit point. The total uncertainty after the likelihood fit remains similar to the PreFit uncertainty, as the sensitivity to the WCs is largely driven by the uncertainties in the production rates, which are only weakly constrained by the fit. We combine all years of data taking prior to the fit but also verified that we obtain compatible results when fitting each data-taking period individually.

JHEP03(2026)140

In order to find the best fit value of the WCs, we calculate the log-likelihood ratio of the EFT prediction and the SM hypothesis as a function of the WCs and evaluate the difference

$$-2\Delta \ln L(\vec{c}, \vec{\nu}) = -2(\ln L(\vec{c}, \vec{\nu}) - \ln L_{\text{MLE}}) = q, \tag{8.1}$$

where $\vec{c}$ are the WCs, $\vec{\nu}$ are the nuisance parameters, L is the profiled likelihood ratio and L_{MLE} is its maximum value. The likelihood is built from the distributions after fitting the nuisance parameters and contains the contributions from all SRs. Using a goodness-of-fit test based on the saturated-model likelihood [81] with 1000 toy experiments, as implemented in COMBINE, we obtain a p-value of 85% for the fit shown in figure 6. The difference of the likelihood under the SM hypothesis, $L(\vec{c} = 0, \vec{\nu})$, and the best fit is $-2(\ln L(\vec{c} = 0, \vec{\nu}) - \ln L_{\text{MLE}}) = 2.5$. Figure 7 shows the best fit values and the confidence intervals for all WCs. It contains results where other WCs are fixed to zero ('fixed') as well as those with other WCs floating in the fit ('profiled'). Figures 8 and 9 show the two-dimensional likelihood scans as functions of the light- and heavy-quark flavour couplings for the fixed and profiled scenarios. Figure 10 shows the limits of the new physics energy scale Λ for each WC. These limits are obtained via $\Lambda = \sqrt{c_i/c(q = 3.84)}$, where c_i is a fixed value and $c(q = 3.84)$ corresponds to the value of the WC at $q = -2\Delta \ln L = 3.84$. For each WC, the least stringent limit on Λ is chosen for display. In the asymptotic approximation, the intervals from the crossing points of q at 1 and 3.84 correspond to the 68 and 95% confidence-level (CL) limits. In the quadratic EFT model, however, Wilks' theorem is not guaranteed to hold for cases where sizeable quadratic contributions are present [82]. Only the operators c_W and $c_{\widetilde{W}}$ show sizable quadratic contributions, such that for all flavour dependent WCs, fits including only linear terms yield results consistent with those from the full EFT model and the violation of Wilks' theorem has little impact.

Overall, we observe consistency with the SM within the uncertainties. This is further verified by extracting the production cross sections of the $\mathrm{t\bar{t}Z}$, WZ, and ZZ processes with all WCs set to zero. All are compatible with the SM predictions and dedicated measurements [83, 84] within one standard deviation. Compared to the SM prediction, the WZ and ZZ cross sections are measured 5% lower and 10% higher, respectively. This effect is compatible with the slight deviations from zero in the fits of $c_{\varphi q}^{(3)(11+22)}$ and $c_{\varphi q}^{(3)(33)}$ as presented in figures 8 and 9.

The WCs $c_{\varphi q}^{(-)(11+22)}$, $c_{\varphi q}^{(-)(33)}$, $c_{\varphi u}^{(11+22)}$, $c_{\varphi u}^{(33)}$, $c_{\varphi d}^{(11+22)}$, and $c_{\varphi d}^{(33)}$ are constrained by the combination of processes that are sensitive to the light- and heavy-quark generations. The effects of $c_{\varphi u}^{(33)}$ and $c_{\varphi q}^{(-)(33)}$ are largely correlated and cannot be fully disentangled in a fit with all EFT parameters. Thus, both parameters show different sizes of uncertainties comparing the fixed and profiled versions of the fit in figure 7. In addition, cancellations between $c_{\varphi u}^{(33)}$ and $c_{\varphi q}^{(-)(33)}$ and the interplay between the linear and quadratic EFT terms cause a secondary minimum in the two-dimensional likelihood scan of $c_{\varphi u}^{(11+22)}$ and $c_{\varphi u}^{(33)}$ along the $c_{\varphi u}^{(33)}$ axis in figure 9 (middle left). Some WCs, especially c_W and $c_{\widetilde{W}}$, are measured close to zero, which reflects the slight deficit in the WZ contribution and the fact that parameters with large quadratic terms can only increase the event yield.

Variations of $c_{\varphi q}^{(3)(11+22)}$ change the coupling of the W boson to quarks and can be thoroughly probed in WZ production. The coupling described by $c_{\varphi q}^{(3)(33)}$ cannot be precisely

JHEP03(2026)140

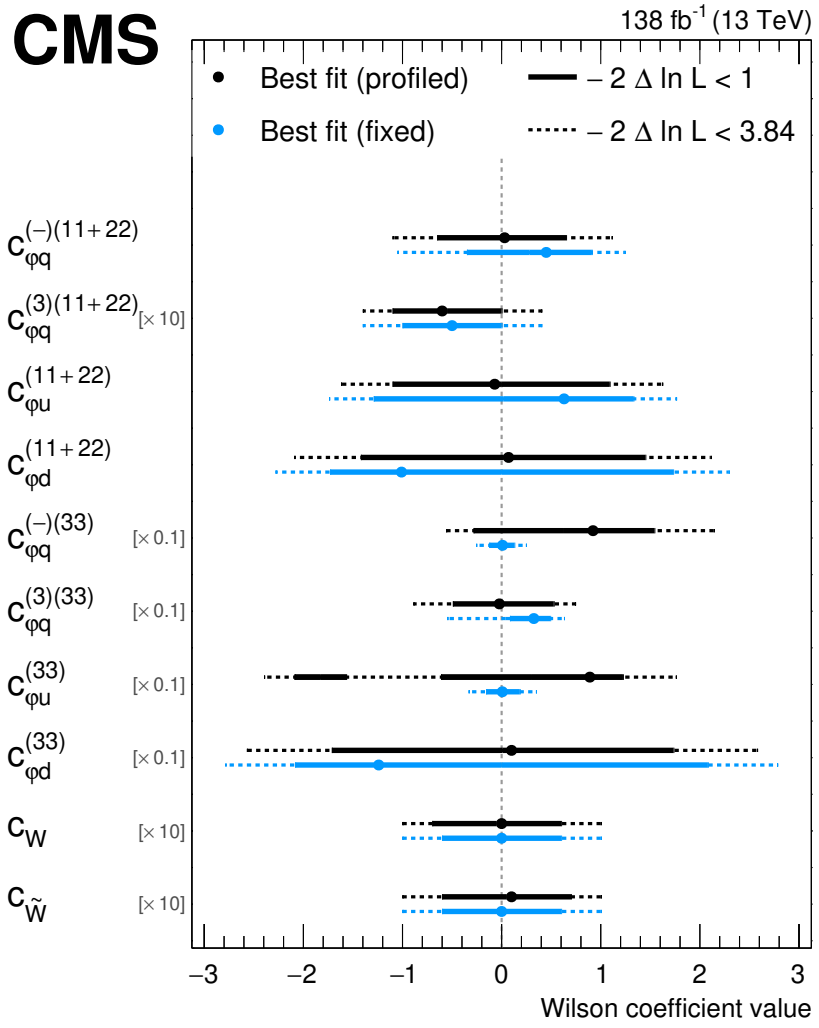

Figure 7. Summary of the limits obtained for the Wilson coefficients $c_{\varphi q}^{(-)(11+22)}$, $c_{\varphi q}^{(3)(11+22)}$, $c_{\varphi u}^{(11+22)}$, $c_{\varphi d}^{(11+22)}$, $c_{\varphi q}^{(-)(33)}$, $c_{\varphi q}^{(3)(33)}$, $c_{\varphi u}^{(33)}$, $c_{\varphi d}^{(33)}$, c_W, and $c_{\widetilde{W}}$. Shown are the best fit points and limits for scans where other Wilson coefficients are fixed to zero ('fixed') or are allowed to float ('profiled'). The points where the difference $-2\Delta \ln L$ with respect to the best fit increases by 1 and 3.84 are shown as horizontal error bars. These points correspond to the 68 and 95% CL limits in the asymptotic approximation. For each Wilson coefficient value, the EFT energy scale is assumed to be $\Lambda = 1$ TeV. For better visibility, the heavy quark couplings are multiplied by a factor of 0.1 and $c_{\varphi q}^{(3)(11+22)}$, c_W, as well as $c_{\widetilde{W}}$ are multiplied by 10.

probed with the setup in this analysis. There is some sensitivity from the Z-b vertex in ZZ production but to probe this coupling more precisely, a vertex with a heavy quark and W boson is needed. Furthermore, this vertex must be a production vertex. Even though such a vertex exists in the top quark decays of the $t\bar{t}Z$ production, it does not add sensitivity to $c_{\varphi q}^{(3)(33)}$ because it only alters the top quark decay and not the production cross section. It was verified that a simple angular analysis of the top quark decay products does not add sensitivity. Compared to another analysis focusing on associated $t\bar{t}$ production [12], similar

JHEP03(2026)140

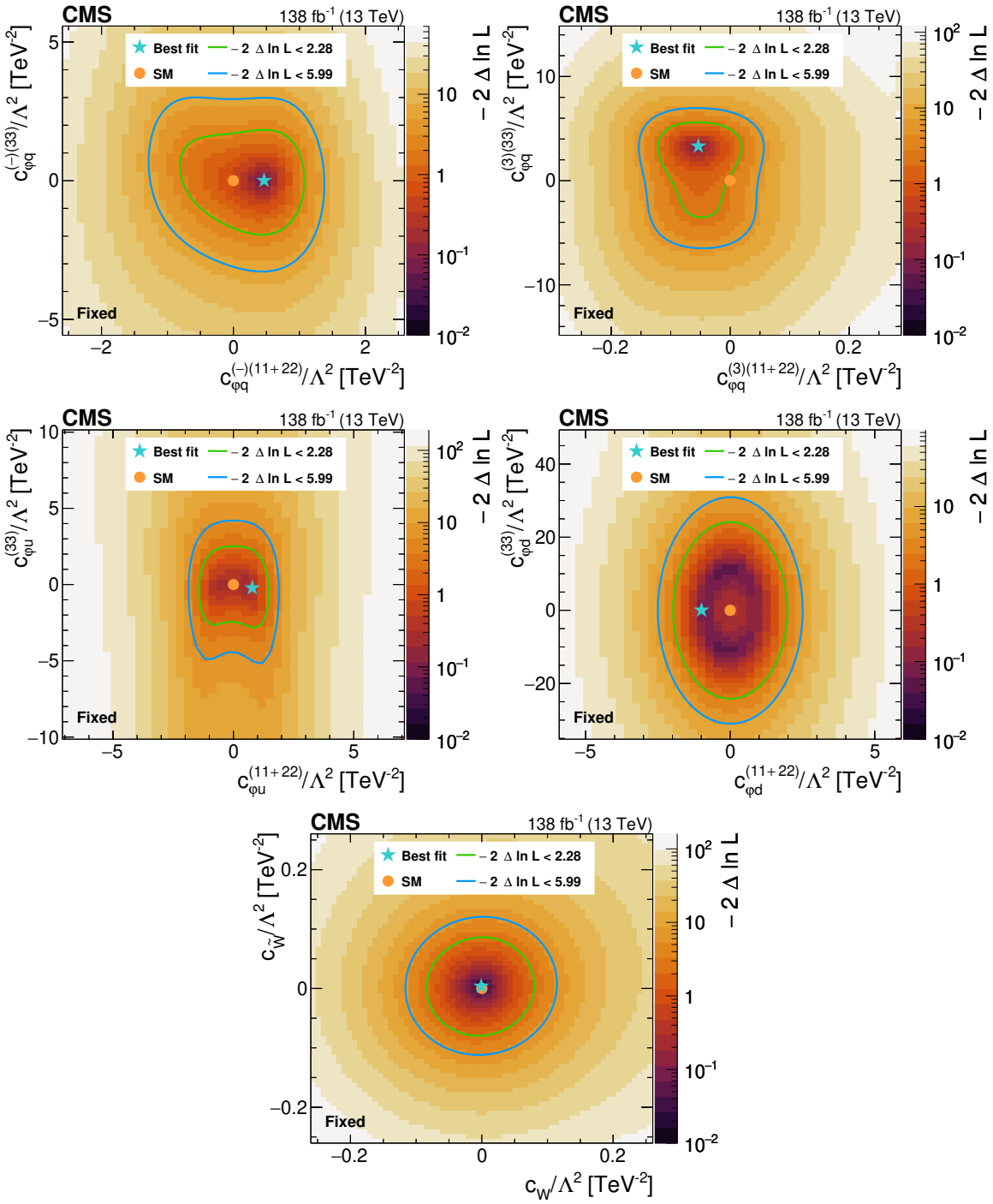

Figure 8. Likelihood as a function of the Wilson coefficients $c_{\varphi q}^{(-)(11+22)}$ and $c_{\varphi q}^{(-)(33)}$ (upper left), $c_{\varphi q}^{(3)(11+22)}$ and $c_{\varphi q}^{(3)(33)}$ (upper right), $c_{\varphi u}^{(11+22)}$ and $c_{\varphi u}^{(33)}$ (middle left), $c_{\varphi d}^{(11+22)}$ and $c_{\varphi d}^{(33)}$ (middle right), as well as c_W and $c_{\widetilde{W}}$ (lower). All Wilson coefficients that are not scanned are fixed to zero. The best fit value is shown with a marker and the coloured lines correspond to the crossing points of $-2\Delta \ln L$ at 2.28 and 5.99, which correspond to the 68 and 95% CL limits in the asymptotic approximation.

JHEP03(2026)140

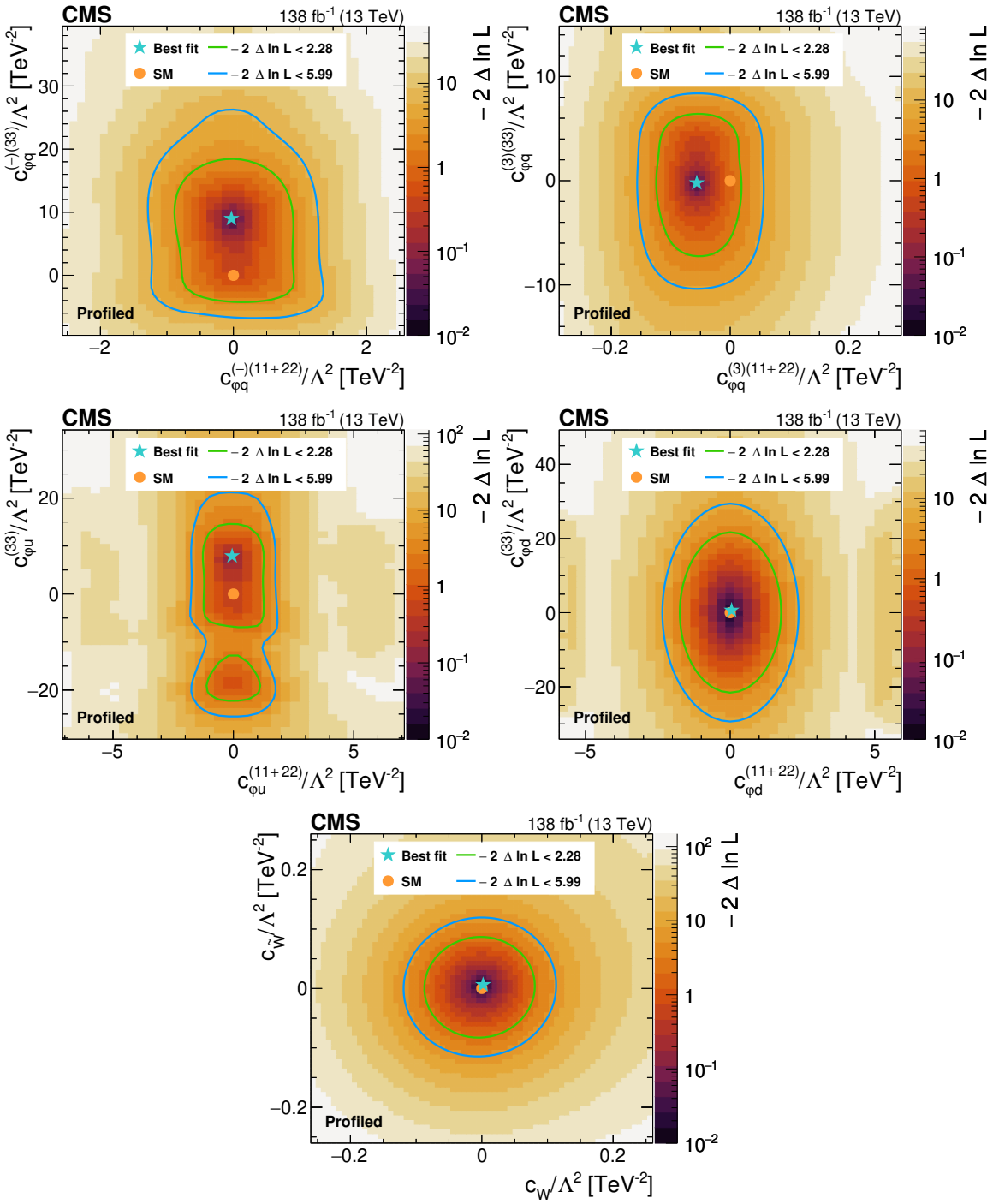

Figure 9. Likelihood as a function of the Wilson coefficients $c_{\varphi q}^{(-)(11+22)}$ and $c_{\varphi q}^{(-)(33)}$ (upper left), $c_{\varphi q}^{(3)(11+22)}$ and $c_{\varphi q}^{(3)(33)}$ (upper right), $c_{\varphi u}^{(11+22)}$ and $c_{\varphi u}^{(33)}$ (middle left), $c_{\varphi d}^{(11+22)}$ and $c_{\varphi d}^{(33)}$ (middle right), as well as c_W and $c_{\widetilde{W}}$ (lower). Other Wilson coefficients are allowed to float in the fit. The best fit value is shown with a marker and the coloured lines correspond to the crossing points of $-2\Delta \ln L$ at 2.28 and 5.99, which correspond to the 68 and 95% CL limits in the asymptotic approximation.

JHEP03(2026)140

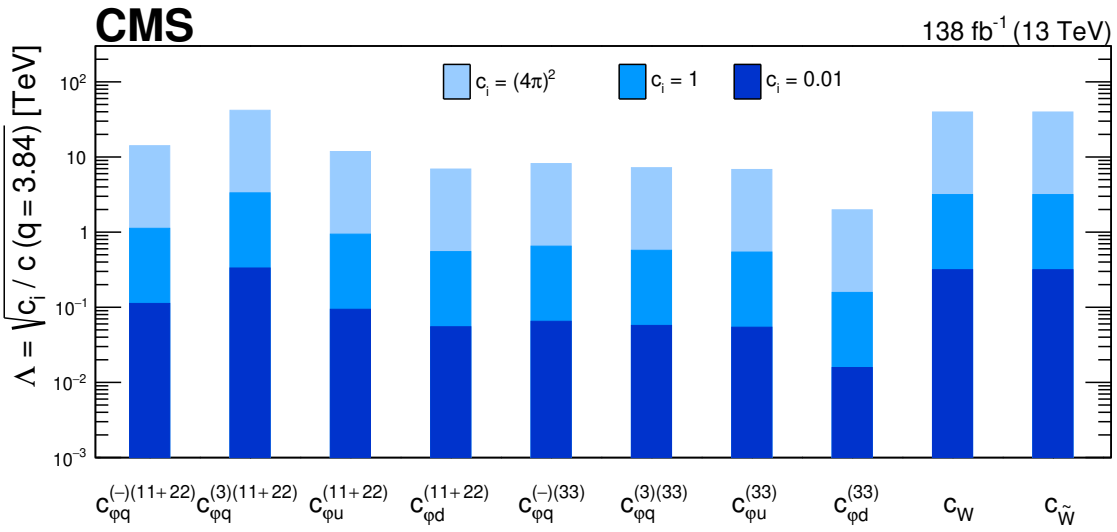

Figure 10. Summary of the limits in the energy scale Λ obtained from the limits on the Wilson coefficients $c_{\varphi q}^{(-)(11+22)}$, $c_{\varphi q}^{(3)(11+22)}$, $c_{\varphi u}^{(11+22)}$, $c_{\varphi d}^{(11+22)}$, $c_{\varphi q}^{(-)(33)}$, $c_{\varphi q}^{(3)(33)}$, $c_{\varphi u}^{(33)}$, $c_{\varphi d}^{(33)}$, c_W, and $c_{\widetilde{W}}$. Shown are limits for scans where other Wilson coefficients are fixed to zero. The limit on Λ is calculated from the Wilson coefficient value at $q = -2\Delta \ln L = 3.84$, which corresponds to the 95% CL limit in the asymptotic approximation. The least stringent limit is chosen for each Wilson coefficient and limits are shown for three scenarios of c_i.

sensitivity is obtained to $c_{\varphi q}^{(-)(33)}$, when fixing other WCs to zero. Compared to an analysis focusing on light quarks [85], weaker limits in $c_{\varphi q}^{(-)(11+22)}$ but comparable limits in $c_{\varphi q}^{(3)(11+22)}$ are observed. Global fits including EW precision data can further constrain $c_{\varphi q}^{(-)(11+22)}$ and $c_{\varphi q}^{(3)(11+22)}$ but obtain similar limits for c_W [86, 87]. However, the presented analysis simultaneously constrains possible flavour differences, which are usually not considered in EFT measurements. The coefficients c_W and $c_{\widetilde{W}}$ can be constrained by the measurement of the WZ process, which can feature a WWZ vertex. Dedicated analyses reach higher sensitivity to these couplings [84, 88].

9 Summary

An analysis of the flavour structures in effective field theory (EFT) couplings has been presented, considering the electroweak coupling to quarks of different generations in the processes $\mathrm{t\bar{t}Z}$, WZ, and ZZ. Proton-proton collision data, collected at $\sqrt{s} = 13\,\mathrm{TeV}$ in 2016–2018 by the CMS detector and corresponding to an integrated luminosity of $138\,\mathrm{fb}^{-1}$ were analysed. For the first time, the flavour structures of the Z-quark couplings are disentangled by simultaneously probing the light- and heavy-quark couplings in different processes. The measured Wilson coefficients are compatible with the standard model hypothesis within their uncertainties and corresponding limits are placed using one- and two-dimensional scans of the profiled likelihood test statistic. Extracting the EFT parameters from multiple processes simultaneously makes it possible to correctly correlate EFT effects of the three processes that are often important backgrounds of each other. Thus, these results contribute to a more

JHEP03(2026)140

comprehensive EFT interpretation that preserves correlations in combinations or global fits, rather than focusing solely on individual processes.

Acknowledgments

We congratulate our colleagues in the CERN accelerator departments for the excellent performance of the LHC and thank the technical and administrative staffs at CERN and at other CMS institutes for their contributions to the success of the CMS effort. In addition, we gratefully acknowledge the computing centres and personnel of the Worldwide LHC Computing Grid and other centres for delivering so effectively the computing infrastructure essential to our analyses. Finally, we acknowledge the enduring support for the construction and operation of the LHC, the CMS detector, and the supporting computing infrastructure provided by the following funding agencies: SC (Armenia), BMBWF and FWF (Austria); FNRS and FWO (Belgium); CNPq, CAPES, FAPERJ, FAPERGS, and FAPESP (Brazil); MES and BNSF (Bulgaria); CERN; CAS, MoST, and NSFC (China); MINCIENCIAS (Colombia); MSES and CSF (Croatia); RIF (Cyprus); SENESCYT (Ecuador); ERC PRG, RVTT3 and MoER TK202 (Estonia); Academy of Finland, MEC, and HIP (Finland); CEA and CNRS/IN2P3 (France); SRNSF (Georgia); BMBF, DFG, and HGF (Germany); GSRI (Greece); NKFIH (Hungary); DAE and DST (India); IPM (Iran); SFI (Ireland); INFN (Italy); MSIT and NRF (Republic of Korea); MES (Latvia); LMTLT (Lithuania); MOE and UM (Malaysia); BUAP, CINVESTAV, CONACYT, LNS, SEP, and UASLP-FAI (Mexico); MOS (Montenegro); MBIE (New Zealand); PAEC (Pakistan); MES and NSC (Poland); FCT (Portugal); MESTD (Serbia); MICIU/AEI and PCTI (Spain); MOSTR (Sri Lanka); Swiss Funding Agencies (Switzerland); MST (Taipei); MHESI and NSTDA (Thailand); TUBITAK and TENMAK (Türkiye); NASU (Ukraine); STFC (U.K.); DOE and NSF (U.S.A.).

Individuals have received support from the Marie-Curie programme and the European Research Council and Horizon 2020 Grant, contract Nos. 675440, 724704, 752730, 758316, 765710, 824093, 101115353, 101002207, 101001205, and COST Action CA16108 (European Union); the Leventis Foundation; the Alfred P. Sloan Foundation; the Alexander von Humboldt Foundation; the Science Committee, project no. 22rl-037 (Armenia); the Fonds pour la Formation à la Recherche dans l'Industrie et dans l'Agriculture (FRIA-Belgium); the Beijing Municipal Science & Technology Commission, No. Z191100007219010, the Fundamental Research Funds for the Central Universities, the Ministry of Science and Technology of China under Grant No. 2023YFA1605804, and the Natural Science Foundation of China under Grant No. 12061141002 (China); the Ministry of Education, Youth and Sports (MEYS) of the Czech Republic; the Shota Rustaveli National Science Foundation, grant FR-22-985 (Georgia); the Deutsche Forschungsgemeinschaft (DFG), among others, under Germany's Excellence Strategy – EXC 2121 "Quantum Universe" – 390833306, and under project number 400140256 – GRK2497; the Hellenic Foundation for Research and Innovation (HFRI), Project Number 2288 (Greece); the Hungarian Academy of Sciences, the New National Excellence Program – ÚNKP, the NKFIH research grants K 131991, K 133046, K 138136, K 143460, K 143477, K 146913, K 146914, K 147048, 2020-2.2.1-ED-2021-00181, TKP2021-NKTA-64, and 2021-4.1.2-NEMZ_KI-2024-00036 (Hungary); the Council of Science and Industrial Research, India; ICSC – National Research Centre for High Performance Computing, Big

JHEP03(2026)140

Data and Quantum Computing, FAIR – Future Artificial Intelligence Research, and CUP I53D23001070006 (Mission 4 Component 1), funded by the NextGenerationEU program (Italy); the Latvian Council of Science; the Ministry of Education and Science, project no. 2022/WK/14, and the National Science Center, contracts Opus 2021/41/B/ST2/01369 and 2021/43/B/ST2/01552 (Poland); the Fundação para a Ciência e a Tecnologia, grant CEECIND/01334/2018 (Portugal); the National Priorities Research Program by Qatar National Research Fund; MICIU/AEI/10.13039/501100011033, ERDF/EU, "European Union NextGenerationEU/PRTR", and Programa Severo Ochoa del Principado de Asturias (Spain); the Chulalongkorn Academic into Its 2nd Century Project Advancement Project, and the National Science, Research and Innovation Fund via the Program Management Unit for Human Resources & Institutional Development, Research and Innovation, grant B39G680009 (Thailand); the Kavli Foundation; the Nvidia Corporation; the SuperMicro Corporation; the Welch Foundation, contract C-1845; and the Weston Havens Foundation (U.S.A.).

Data Availability Statement. Release and preservation of data used by the CMS Collaboration as the basis for publications is guided by the CMS data preservation, re-use and open access policy.

Code Availability Statement. The CMS core software is publicly available on GitHub.

References

[1] C.P. Burgess, *Introduction to Effective Field Theory*, Cambridge University Press (2020) [DOI:10.1017/9781139048040] [INSPIRE].

[2] W. Buchmüller and D. Wyler, *Effective Lagrangian Analysis of New Interactions and Flavor Conservation*, *Nucl. Phys. B* **268** (1986) 621 [INSPIRE].

[3] I. Brivio and M. Trott, *The Standard Model as an Effective Field Theory*, *Phys. Rept.* **793** (2019) 1 [arXiv:1706.08945] [INSPIRE].

[4] G.F. Giudice, C. Grojean, A. Pomarol and R. Rattazzi, *The Strongly-Interacting Light Higgs*, *JHEP* **06** (2007) 045 [hep-ph/0703164] [INSPIRE].

[5] B. Grzadkowski, M. Iskrzynski, M. Misiak and J. Rosiek, *Dimension-Six Terms in the Standard Model Lagrangian*, *JHEP* **10** (2010) 085 [arXiv:1008.4884] [INSPIRE].

[6] A. Helset and A. Kobach, *Baryon Number, Lepton Number, and Operator Dimension in the SMEFT with Flavor Symmetries*, *Phys. Lett. B* **800** (2020) 135132 [arXiv:1909.05853] [INSPIRE].

[7] ATLAS collaboration, *Inclusive and differential cross-section measurements of $t\bar{t}Z$ production in pp collisions at $\sqrt{s} = 13$ TeV with the ATLAS detector, including EFT and spin-correlation interpretations*, *JHEP* **07** (2024) 163 [arXiv:2312.04450] [INSPIRE].

[8] ATLAS collaboration, *Measurements of inclusive and differential cross-sections of $t\bar{t}\gamma$ production in pp collisions at $\sqrt{s} = 13$ TeV with the ATLAS detector*, *JHEP* **10** (2024) 191 [arXiv:2403.09452] [INSPIRE].

JHEP03(2026)140

[9] CMS collaboration, *Probing effective field theory operators in the associated production of top quarks with a Z boson in multilepton final states at* $\sqrt{s} = 13$ *TeV*, *JHEP* **12** (2021) 083 [arXiv:2107.13896] [INSPIRE].

[10] CMS collaboration, *Search for new physics using effective field theory in 13 TeV pp collision events that contain a top quark pair and a boosted Z or Higgs boson*, *Phys. Rev. D* **108** (2023) 032008 [arXiv:2208.12837] [INSPIRE].

[11] CMS collaboration, *Search for new physics in top quark production with additional leptons in proton-proton collisions at* $\sqrt{s} = 13$ *TeV using effective field theory*, *JHEP* **03** (2021) 095 [arXiv:2012.04120] [INSPIRE].

[12] CMS collaboration, *Search for physics beyond the standard model in top quark production with additional leptons in the context of effective field theory*, *JHEP* **12** (2023) 068 [arXiv:2307.15761] [INSPIRE].

[13] S. Bißmann, C. Grunwald, G. Hiller and K. Kröninger, *Top and Beauty synergies in SMEFT-fits at present and future colliders*, *JHEP* **06** (2021) 010 [arXiv:2012.10456] [INSPIRE].

[14] S. Bruggisser, R. Schäfer, D. van Dyk and S. Westhoff, *The Flavor of UV Physics*, *JHEP* **05** (2021) 257 [arXiv:2101.07273] [INSPIRE].

[15] ATLAS collaboration, *Search for flavour-changing neutral current top-quark decays* $t \to qZ$ *in proton-proton collisions at* $\sqrt{s} = 13$ *TeV with the ATLAS detector*, *JHEP* **07** (2018) 176 [arXiv:1803.09923] [INSPIRE].

[16] ATLAS collaboration, *Search for flavour-changing neutral-current interactions of a top quark and a gluon in pp collisions at* $\sqrt{s} = 13$ *TeV with the ATLAS detector*, *Eur. Phys. J. C* **82** (2022) 334 [arXiv:2112.01302] [INSPIRE].

[17] ATLAS collaboration, *Search for flavour-changing neutral-current couplings between the top quark and the photon with the ATLAS detector at* $\sqrt{s} = 13$ *TeV*, *Phys. Lett. B* **842** (2023) 137379 [*Erratum ibid.* **847** (2024) 138286] [arXiv:2205.02537] [INSPIRE].

[18] CMS collaboration, *Search for new physics in top quark production in dilepton final states in proton-proton collisions at* $\sqrt{s} = 13$ *TeV*, *Eur. Phys. J. C* **79** (2019) 886 [arXiv:1903.11144] [INSPIRE].

[19] CMS collaboration, *Measurement of the inclusive and differential* $t\bar{t}\gamma$ *cross sections in the dilepton channel and effective field theory interpretation in proton-proton collisions at* $\sqrt{s} = 13$ *TeV*, *JHEP* **05** (2022) 091 [arXiv:2201.07301] [INSPIRE].

[20] *HEPData record for this analysis*, DOI:10.17182/hepdata.157849 (2025).

[21] CMS collaboration, *The CMS Experiment at the CERN LHC*, 2008 *JINST* **3** S08004 [INSPIRE].

[22] CMS Tracker Group collaboration, *The CMS Phase-1 Pixel Detector Upgrade*, 2021 *JINST* **16** P02027 [arXiv:2012.14304] [INSPIRE].

[23] CMS collaboration, *Performance of the CMS Level-1 trigger in proton-proton collisions at* $\sqrt{s} = 13$ *TeV*, 2020 *JINST* **15** P10017 [arXiv:2006.10165] [INSPIRE].

[24] CMS collaboration, *The CMS trigger system*, 2017 *JINST* **12** P01020 [arXiv:1609.02366] [INSPIRE].

[25] CMS collaboration, *Performance of the CMS high-level trigger during LHC Run 2*, 2024 *JINST* **19** P11021 [arXiv:2410.17038] [INSPIRE].

JHEP03(2026)140

[26] J. Alwall et al., *The automated computation of tree-level and next-to-leading order differential cross sections, and their matching to parton shower simulations*, *JHEP* **07** (2014) 079 [arXiv:1405.0301] [INSPIRE].

[27] S. Frixione and B.R. Webber, *Matching NLO QCD computations and parton shower simulations*, *JHEP* **06** (2002) 029 [hep-ph/0204244] [INSPIRE].

[28] T. Melia, P. Nason, R. Röntsch and G. Zanderighi, W^+W^-, *WZ and ZZ production in the POWHEG BOX*, *JHEP* **11** (2011) 078 [arXiv:1107.5051] [INSPIRE].

[29] P. Nason and G. Zanderighi, W^+W^-, *WZ and ZZ production in the POWHEG-BOX-V2*, *Eur. Phys. J. C* **74** (2014) 2702 [arXiv:1311.1365] [INSPIRE].

[30] O. Mattelaer, *On the maximal use of Monte Carlo samples: re-weighting events at NLO accuracy*, *Eur. Phys. J. C* **76** (2016) 674 [arXiv:1607.00763] [INSPIRE].

[31] I. Brivio, Y. Jiang and M. Trott, *The SMEFTsim package, theory and tools*, *JHEP* **12** (2017) 070 [arXiv:1709.06492] [INSPIRE].

[32] I. Brivio, *SMEFTsim 3.0 — a practical guide*, *JHEP* **04** (2021) 073 [arXiv:2012.11343] [INSPIRE].

[33] P. Nason, *A new method for combining NLO QCD with shower Monte Carlo algorithms*, *JHEP* **11** (2004) 040 [hep-ph/0409146] [INSPIRE].

[34] S. Frixione, P. Nason and C. Oleari, *Matching NLO QCD computations with Parton Shower simulations: the POWHEG method*, *JHEP* **11** (2007) 070 [arXiv:0709.2092] [INSPIRE].

[35] S. Alioli, P. Nason, C. Oleari and E. Re, *A general framework for implementing NLO calculations in shower Monte Carlo programs: the POWHEG BOX*, *JHEP* **06** (2010) 043 [arXiv:1002.2581] [INSPIRE].

[36] S. Frixione, P. Nason and G. Ridolfi, *A positive-weight next-to-leading-order Monte Carlo for heavy flavour hadroproduction*, *JHEP* **09** (2007) 126 [arXiv:0707.3088] [INSPIRE].

[37] H.B. Hartanto, B. Jäger, L. Reina and D. Wackeroth, *Higgs boson production in association with top quarks in the POWHEG BOX*, *Phys. Rev. D* **91** (2015) 094003 [arXiv:1501.04498] [INSPIRE].

[38] S. Alioli, P. Nason, C. Oleari and E. Re, *NLO single-top production matched with shower in POWHEG: s- and t-channel contributions*, *JHEP* **09** (2009) 111 [*Erratum ibid.* **02** (2010) 011] [arXiv:0907.4076] [INSPIRE].

[39] E. Re, *Single-top Wt-channel production matched with parton showers using the POWHEG method*, *Eur. Phys. J. C* **71** (2011) 1547 [arXiv:1009.2450] [INSPIRE].

[40] T. Sjöstrand et al., *An introduction to PYTHIA 8.2*, *Comput. Phys. Commun.* **191** (2015) 159 [arXiv:1410.3012] [INSPIRE].

[41] J.M. Campbell and R.K. Ellis, *An update on vector boson pair production at hadron colliders*, *Phys. Rev. D* **60** (1999) 113006 [hep-ph/9905386] [INSPIRE].

[42] J.M. Campbell, R.K. Ellis and C. Williams, *Vector Boson Pair Production at the LHC*, *JHEP* **07** (2011) 018 [arXiv:1105.0020] [INSPIRE].

[43] J.M. Campbell, R.K. Ellis and W.T. Giele, *A Multi-Threaded Version of MCFM*, *Eur. Phys. J. C* **75** (2015) 246 [arXiv:1503.06182] [INSPIRE].

[44] CMS collaboration, *Extraction and validation of a new set of CMS PYTHIA8 tunes from underlying-event measurements*, *Eur. Phys. J. C* **80** (2020) 4 [arXiv:1903.12179] [INSPIRE].

JHEP03(2026)140

[45] R. Frederix and S. Frixione, *Merging meets matching in MC@NLO*, *JHEP* **12** (2012) 061 [arXiv:1209.6215] [INSPIRE].

[46] J. Alwall et al., *Comparative study of various algorithms for the merging of parton showers and matrix elements in hadronic collisions*, *Eur. Phys. J. C* **53** (2008) 473 [arXiv:0706.2569] [INSPIRE].

[47] NNPDF collaboration, *Parton distributions from high-precision collider data*, *Eur. Phys. J. C* **77** (2017) 663 [arXiv:1706.00428] [INSPIRE].

[48] GEANT4 collaboration, *GEANT4 — A Simulation Toolkit*, *Nucl. Instrum. Meth. A* **506** (2003) 250 [INSPIRE].

[49] J. Allison et al., *Geant4 developments and applications*, *IEEE Trans. Nucl. Sci.* **53** (2006) 270 [INSPIRE].

[50] CMS collaboration, *Particle-flow reconstruction and global event description with the CMS detector*, 2017 *JINST* **12** P10003 [arXiv:1706.04965] [INSPIRE].

[51] D. Contardo et al., *Technical Proposal for the Phase-II Upgrade of the CMS Detector*, CERN-LHCC-2015-010 (2015) [DOI:10.17181/CERN.VU8I.D59J] [INSPIRE].

[52] CMS collaboration, *Performance of missing transverse momentum reconstruction in proton-proton collisions at* $\sqrt{s} = 13$ *TeV using the CMS detector*, 2019 *JINST* **14** P07004 [arXiv:1903.06078] [INSPIRE].

[53] CMS collaboration, *Electron and photon reconstruction and identification with the CMS experiment at the CERN LHC*, 2021 *JINST* **16** P05014 [arXiv:2012.06888] [INSPIRE].

[54] CMS collaboration, *Performance of the CMS muon detector and muon reconstruction with proton-proton collisions at* $\sqrt{s} = 13$ *TeV*, 2018 *JINST* **13** P06015 [arXiv:1804.04528] [INSPIRE].

[55] CMS collaboration, *Observation of four top quark production in proton-proton collisions at* $\sqrt{s} = 13$ *TeV*, *Phys. Lett. B* **847** (2023) 138290 [arXiv:2305.13439] [INSPIRE].

[56] CMS collaboration, *Muon identification using multivariate techniques in the CMS experiment in proton-proton collisions at* $\sqrt{s} = 13$ *TeV*, 2024 *JINST* **19** P02031 [arXiv:2310.03844] [INSPIRE].

[57] M. Cacciari, G.P. Salam and G. Soyez, *The anti-*k_t *jet clustering algorithm*, *JHEP* **04** (2008) 063 [arXiv:0802.1189] [INSPIRE].

[58] M. Cacciari, G.P. Salam and G. Soyez, *FastJet User Manual*, *Eur. Phys. J. C* **72** (2012) 1896 [arXiv:1111.6097] [INSPIRE].

[59] CMS collaboration, *Jet energy scale and resolution in the CMS experiment in pp collisions at 8 TeV*, 2017 *JINST* **12** P02014 [arXiv:1607.03663] [INSPIRE].

[60] CMS collaboration, *Performance of b tagging algorithms in proton-proton collisions at 13 TeV with Phase 1 CMS detector*, CMS Detector Performance Note CMS-DP-2018-033 (2018).

[61] E. Bols et al., *Jet Flavour Classification Using DeepJet*, 2020 *JINST* **15** P12012 [arXiv:2008.10519] [INSPIRE].

[62] PARTICLE DATA GROUP collaboration, *Review of particle physics*, *Phys. Rev. D* **110** (2024) 030001 [INSPIRE].

[63] CMS collaboration, *Evidence for associated production of a Higgs boson with a top quark pair in final states with electrons, muons, and hadronically decaying* τ *leptons at* $\sqrt{s} = 13$ *TeV*, *JHEP* **08** (2018) 066 [arXiv:1803.05485] [INSPIRE].

JHEP03(2026)140

[64] CMS collaboration, *Measurement of the Higgs boson production rate in association with top quarks in final states with electrons, muons, and hadronically decaying tau leptons at* $\sqrt{s} = 13$ *TeV*, *Eur. Phys. J. C* **81** (2021) 378 [arXiv:2011.03652] [INSPIRE].

[65] CMS collaboration, *Identification of heavy-flavour jets with the CMS detector in pp collisions at 13 TeV*, 2018 *JINST* **13** P05011 [arXiv:1712.07158] [INSPIRE].

[66] CMS collaboration, *Pileup mitigation at CMS in 13 TeV data*, 2020 *JINST* **15** P09018 [arXiv:2003.00503] [INSPIRE].

[67] CMS collaboration, *Precision luminosity measurement in proton-proton collisions at* $\sqrt{s} = 13$ *TeV in 2015 and 2016 at CMS*, *Eur. Phys. J. C* **81** (2021) 800 [arXiv:2104.01927] [INSPIRE].

[68] CMS collaboration, *CMS luminosity measurement for the 2017 data-taking period at* $\sqrt{s} = 13$ *TeV*, CMS-PAS-LUM-17-004 (2018) [INSPIRE].

[69] CMS collaboration, *CMS luminosity measurement for the 2018 data-taking period at* $\sqrt{s} = 13$ *TeV*, CMS-PAS-LUM-18-002 (2019) [INSPIRE].

[70] NNPDF collaboration, *Parton distributions for the LHC Run II*, *JHEP* **04** (2015) 040 [arXiv:1410.8849] [INSPIRE].

[71] CMS collaboration, *Measurement of the cross section of top quark-antiquark pair production in association with a W boson in proton-proton collisions at* $\sqrt{s} = 13$ *TeV*, *JHEP* **07** (2023) 219 [arXiv:2208.06485] [INSPIRE].

[72] A. Kulesza et al., *Associated top quark pair production with a heavy boson: differential cross sections at NLO+NNLL accuracy*, *Eur. Phys. J. C* **80** (2020) 428 [arXiv:2001.03031] [INSPIRE].

[73] CMS collaboration, *Inclusive and differential cross section measurements of single top quark production in association with a Z boson in proton-proton collisions at* $\sqrt{s} = 13$ *TeV*, *JHEP* **02** (2022) 107 [arXiv:2111.02860] [INSPIRE].

[74] CMS collaboration, *Measurements of production cross sections of WZ and same-sign WW boson pairs in association with two jets in proton-proton collisions at* $\sqrt{s} = 13$ *TeV*, *Phys. Lett. B* **809** (2020) 135710 [arXiv:2005.01173] [INSPIRE].

[75] F. Cascioli et al., *ZZ production at hadron colliders in NNLO QCD*, *Phys. Lett. B* **735** (2014) 311 [arXiv:1405.2219] [INSPIRE].

[76] M. Grazzini et al., *NNLO QCD + NLO EW with Matrix+OpenLoops: precise predictions for vector-boson pair production*, *JHEP* **02** (2020) 087 [arXiv:1912.00068] [INSPIRE].

[77] CMS collaboration, *The CMS Statistical Analysis and Combination Tool: Combine*, *Comput. Softw. Big Sci.* **8** (2024) 19 [arXiv:2404.06614] [INSPIRE].

[78] W. Verkerke and D.P. Kirkby, *The RooFit toolkit for data modeling*, *eConf C* **0303241** (2003) MOLT007 [physics/0306116] [INSPIRE].

[79] L. Moneta et al., *The RooStats Project*, *PoS* **ACAT2010** (2010) 057 [arXiv:1009.1003] [INSPIRE].

[80] R.J. Barlow and C. Beeston, *Fitting using finite Monte Carlo samples*, *Comput. Phys. Commun.* **77** (1993) 219 [INSPIRE].

[81] R.D. Cousins, *Lectures on Statistics in Theory: Prelude to Statistics in Practice*, arXiv:1807.05996 [INSPIRE].

JHEP03(2026)140

[82] F.U. Bernlochner, D.C. Fry, S.B. Menary and E. Persson, *Cover your bases: asymptotic distributions of the profile likelihood ratio when constraining effective field theories in high-energy physics*, *SciPost Phys. Core* **6** (2023) 013 [arXiv:2207.01350] [INSPIRE].

[83] CMS collaboration, *Measurements of $pp \to ZZ$ production cross sections and constraints on anomalous triple gauge couplings at $\sqrt{s} = 13$ TeV*, *Eur. Phys. J. C* **81** (2021) 200 [arXiv:2009.01186] [INSPIRE].

[84] CMS collaboration, *Measurement of the inclusive and differential WZ production cross sections, polarization angles, and triple gauge couplings in pp collisions at $\sqrt{s} = 13$ TeV*, *JHEP* **07** (2022) 032 [arXiv:2110.11231] [INSPIRE].

[85] CMS collaboration, *Constraints on standard model effective field theory for a Higgs boson produced in association with W or Z bosons in the $H \to b\bar{b}$ decay channel in proton-proton collisions at $\sqrt{s} = 13$ TeV*, *JHEP* **03** (2025) 114 [arXiv:2411.16907] [INSPIRE].

[86] J. Ellis, C.W. Murphy, V. Sanz and T. You, *Updated Global SMEFT Fit to Higgs, Diboson and Electroweak Data*, *JHEP* **06** (2018) 146 [arXiv:1803.03252] [INSPIRE].

[87] J. Ellis et al., *Top, Higgs, Diboson and Electroweak Fit to the Standard Model Effective Field Theory*, *JHEP* **04** (2021) 279 [arXiv:2012.02779] [INSPIRE].

[88] ATLAS collaboration, *Measurements of $W^+W^-+ \geq 1$ jet production cross-sections in pp collisions at $\sqrt{s} = 13$ TeV with the ATLAS detector*, *JHEP* **06** (2021) 003 [arXiv:2103.10319] [INSPIRE].

JHEP03(2026)140

The CMS collaboration

A. Hayrapetyan[1], V. Makarenko[1], A. Tumasyan[1,a], W. Adam[2], J.W. Andrejkovic[2], L. Benato[2], T. Bergauer[2], M. Dragicevic[2], C. Giordano[2], P.S. Hussain[2], M. Jeitler[2,b], N. Krammer[2], A. Li[2], D. Liko[2], M. Matthewman[2], I. Mikulec[2], J. Schieck[2,b], D. Schwarz[2], R. Schöfbeck[2,b], M. Shooshtari[2], M. Sonawane[2], W. Waltenberger[2], C.-E. Wulz[2,b], T. Janssen[3], H. Kwon[3], D. Ocampo Henao[3], T. Van Laer[3], P. Van Mechelen[3], J. Bierkens[4], N. Breugelmans[4], J. D'Hondt[4], S. Dansana[4], A. De Moor[4], M. Delcourt[4], F. Heyen[4], Y. Hong[4], P. Kashko[4], S. Lowette[4], I. Makarenko[4], D. Müller[4], J. Song[4], S. Tavernier[4], M. Tytgat[4,c], G.P. Van Onsem[4], S. Van Putte[4], D. Vannerom[4], B. Bilin[5], B. Clerbaux[5], A.K. Das[5], I. De Bruyn[5], G. De Lentdecker[5], H. Evard[5], L. Favart[5], P. Gianneios[5], A. Khalilzadeh[5], F.A. Khan[5], A. Malara[5], M.A. Shahzad[5], L. Thomas[5], M. Vanden Bemden[5], C. Vander Velde[5], P. Vanlaer[5], F. Zhang[5], M. De Coen[6], D. Dobur[6], G. Gokbulut[6], J. Knolle[6], L. Lambrecht[6], D. Marckx[6], K. Skovpen[6], N. Van Den Bossche[6], J. van der Linden[6], J. Vandenbroeck[6], L. Wezenbeek[6], S. Bein[7], A. Benecke[7], A. Bethani[7], G. Bruno[7], A. Cappati[7], J. De Favereau De Jeneret[7], C. Delaere[7], A. Giammanco[7], A.O. Guzel[7], V. Lemaitre[7], J. Lidrych[7], P. Malek[7], P. Mastrapasqua[7], S. Turkcapar[7], G.A. Alves[8], M. Barroso Ferreira Filho[8], E. Coelho[8], C. Hensel[8], T. Menezes De Oliveira[8], C. Mora Herrera[8,d], P. Rebello Teles[8], M. Soeiro[8], E.J. Tonelli Manganote[8,e], A. Vilela Pereira[8,d], W.L. Aldá Júnior[9], H. Brandao Malbouisson[9], W. Carvalho[9], J. Chinellato[9,f], M. Costa Reis[9], E.M. Da Costa[9], G.G. Da Silveira[9,g], D. De Jesus Damiao[9], S. Fonseca De Souza[9], R. Gomes De Souza[9], S. S. Jesus[9], T. Laux Kuhn[9,g], M. Macedo[9], K. Mota Amarilo[9], L. Mundim[9], H. Nogima[9], J.P. Pinheiro[9], A. Santoro[9], A. Sznajder[9], M. Thiel[9], F. Torres Da Silva De Araujo[9,h], C.A. Bernardes[10,g], E.M. Gregores[10], B. Lopes Da Costa[10], I. Maietto Silverio[10], P.G. Mercadante[10], S.F. Novaes[10], B. Orzari[10], Sandra S. Padula[10], V. Scheurer[10], T.R. Fernandez Perez Tomei[10], A. Aleksandrov[11], G. Antchev[11], P. Danev[11], R. Hadjiiska[11], P. Iaydjiev[11], M. Misheva[11], M. Shopova[11], G. Sultanov[11], A. Dimitrov[12], L. Litov[12], B. Pavlov[12], P. Petkov[12], A. Petrov[12], S. Keshri[13], D. Laroze[13], S. Thakur[13], W. Brooks[14], T. Cheng[15], T. Javaid[15], L. Wang[15], L. Yuan[15], Z. Hu[16], Z. Liang[16], J. Liu[16], X. Wang[16], G.M. Chen[17,i], H.S. Chen[17,i], M. Chen[17,i], Y. Chen[17], Q. Hou[17], X. Hou[17], F. Iemmi[17], C.H. Jiang[17], A. Kapoor[17,j], H. Liao[17], G. Liu[17], Z.-A. Liu[17,k], J.N. Song[17,k], S. Song[17], J. Tao[17], C. Wang[17,i], J. Wang[17], H. Zhang[17], J. Zhao[17], A. Agapitos[18], Y. Ban[18], A. Carvalho Antunes De Oliveira[18], S. Deng[18], B. Guo[18], Q. Guo[18], C. Jiang[18], A. Levin[18], C. Li[18], Q. Li[18], Y. Mao[18], S. Qian[18], S.J. Qian[18], X. Qin[18], X. Sun[18], D. Wang[18], J. Wang[18], H. Yang[18], M. Zhang[18], Y. Zhao[18], C. Zhou[18], S. Yang[19], Z. You[20], K. Jaffel[21], N. Lu[21], G. Bauer[22,l,m], B. Li[22,n], H. Wang[22], K. Yi[22,o], J. Zhang[22], Y. Li[23], Z. Lin[24], C. Lu[24], M. Xiao[24,p], C. Avila[25], D.A. Barbosa Trujillo[25], A. Cabrera[25], C. Florez[25], J. Fraga[25], J.A. Reyes Vega[25], C. Rendón[26], M. Rodriguez[26], A.A. Ruales Barbosa[26], J.D. Ruiz Alvarez[26], N. Godinovic[27], D. Lelas[27], A. Sculac[27], M. Kovac[28], A. Petkovic[28], T. Sculac[28], P. Bargassa[29], V. Brigljevic[29], B.K. Chitroda[29], D. Ferencek[29], K. Jakovcic[29], A. Starodumov[29], T. Susa[29], A. Attikis[30], K. Christoforou[30], A. Hadjiagapiou[30], C. Leonidou[30], C. Nicolaou[30], L. Paizanos[30], F. Ptochos[30], P.A. Razis[30],

JHEP03(2026)140

H. Rykaczewski[30], H. Saka[30], A. Stepennov[30], M. Finger[31,†], M. Finger Jr.[31], E. Ayala[32], E. Carrera Jarrin[33], A.A. Abdelalim[34,q,r], R. Aly[34,s,t], A. Hussein[35], H. Mohammed[35], M. Abdullah Al-Mashad[35], K. Ehataht[36], M. Kadastik[36], T. Lange[36], C. Nielsen[36], J. Pata[36], M. Raidal[36], N. Seeba[36], L. Tani[36], A. Milieva[37], K. Osterberg[37], M. Voutilainen[37], N. Bin Norjoharuddeen[38], E. Brücken[38], F. Garcia[38], P. Inkaew[38], K.T.S. Kallonen[38], R. Kumar Verma[38], T. Lampén[38], K. Lassila-Perini[38], B. Lehtela[38], S. Lehti[38], T. Lindén[38], N.R. Mancilla Xinto[38], M. Myllymäki[38], M.m. Rantanen[38], S. Saariokari[38], N.T. Toikka[38], J. Tuominiemi[38], H. Kirschenmann[39], P. Luukka[39], H. Petrow[39], M. Besancon[40], F. Couderc[40], M. Dejardin[40], D. Denegri[40], P. Devouge[40], J.L. Faure[40], F. Ferri[40], P. Gaigne[40], S. Ganjour[40], P. Gras[40], G. Hamel de Monchenault[40], M. Kumar[40], V. Lohezic[40], J. Malcles[40], F. Orlandi[40], L. Portales[40], S. Ronchi[40], M.Ö. Sahin[40], A. Savoy-Navarro[40,u], P. Simkina[40], M. Titov[40], M. Tornago[40], F. Beaudette[41], G. Boldrini[41], P. Busson[41], C. Charlot[41], M. Chiusi[41], T.D. Cuisset[41], F. Damas[41], O. Davignon[41], A. De Wit[41], T. Debnath[41], I.T. Ehle[41], B.A. Fontana Santos Alves[41], S. Ghosh[41], A. Gilbert[41], R. Granier de Cassagnac[41], L. Kalipoliti[41], M. Manoni[41], M. Nguyen[41], S. Obraztsov[41], C. Ochando[41], R. Salerno[41], J.B. Sauvan[41], Y. Sirois[41], G. Sokmen[41], L. Urda Gómez[41], A. Zabi[41], A. Zghiche[41], J.-L. Agram[42,v], J. Andrea[42], D. Bloch[42], J.-M. Brom[42], E.C. Chabert[42], C. Collard[42], G. Coulon[42], S. Falke[42], U. Goerlach[42], R. Haeberle[42], A.-C. Le Bihan[42], M. Meena[42], O. Poncet[42], G. Saha[42], P. Vaucelle[42], A. Di Florio[43], D. Amram[44], S. Beauceron[44], B. Blancon[44], G. Boudoul[44], N. Chanon[44], D. Contardo[44], P. Depasse[44], C. Dozen[44,w], H. El Mamouni[44], J. Fay[44], S. Gascon[44], M. Gouzevitch[44], C. Greenberg[44], G. Grenier[44], B. Ille[44], E. Jourd'huy[44], I.B. Laktineh[44], M. Lethuillier[44], B. Massoteau[44], L. Mirabito[44], A. Purohit[44], M. Vander Donckt[44], J. Xiao[44], A. Khvedelidze[45,x], I. Lomidze[45], Z. Tsamalaidze[45,x], V. Botta[46], S. Consuegra Rodríguez[46], L. Feld[46], K. Klein[46], M. Lipinski[46], D. Meuser[46], P. Nattland[46], V. Oppenländer[46], A. Pauls[46], D. Pérez Adán[46], N. Röwert[46], M. Teroerde[46], C. Daumann[47], S. Diekmann[47], A. Dodonova[47], N. Eich[47], D. Eliseev[47], F. Engelke[47], J. Erdmann[47], M. Erdmann[47], B. Fischer[47], T. Hebbeker[47], K. Hoepfner[47], F. Ivone[47], A. Jung[47], N. Kumar[47], M.y. Lee[47], F. Mausolf[47], M. Merschmeyer[47], A. Meyer[47], F. Nowotny[47], A. Pozdnyakov[47], W. Redjeb[47], H. Reithler[47], U. Sarkar[47], V. Sarkisovi[47], A. Schmidt[47], C. Seth[47], A. Sharma[47], J.L. Spah[47], V. Vaulin[47], S. Zaleski[47], M.R. Beckers[48], C. Dziwok[48], G. Flügge[48], N. Hoeflich[48], T. Kress[48], A. Nowack[48], O. Pooth[48], A. Stahl[48], A. Zotz[48], H. Aarup Petersen[49], A. Abel[49], M. Aldaya Martin[49], J. Alimena[49], S. Amoroso[49], Y. An[49], I. Andreev[49], J. Bach[49], S. Baxter[49], M. Bayatmakou[49], H. Becerril Gonzalez[49], O. Behnke[49], A. Belvedere[49], F. Blekman[49,y], K. Borras[49,z], A. Campbell[49], S. Chatterjee[49], L.X. Coll Saravia[49], G. Eckerlin[49], D. Eckstein[49], E. Gallo[49,y], A. Geiser[49], V. Guglielmi[49], M. Guthoff[49], A. Hinzmann[49], L. Jeppe[49], M. Kasemann[49], C. Kleinwort[49], R. Kogler[49], M. Komm[49], D. Krücker[49], W. Lange[49], D. Leyva Pernia[49], K.-Y. Lin[49], K. Lipka[49,aa], W. Lohmann[49,ab], J. Malvaso[49], R. Mankel[49], I.-A. Melzer-Pellmann[49], M. Mendizabal Morentin[49], A.B. Meyer[49], G. Milella[49], K. Moral Figueroa[49], A. Mussgiller[49], L.P. Nair[49], J. Niedziela[49], A. Nürnberg[49], J. Park[49], E. Ranken[49], A. Raspereza[49], D. Rastorguev[49], L. Rygaard[49],

JHEP03(2026)140

M. Scham[49,ac,ad], S. Schnake[49,z], C. Schwanenberger[49,y], P. Schütze[49], D. Selivanova[49], K. Sharko[49], M. Shchedrolosiev[49], D. Stafford[49], M. Torkian[49], F. Vazzoler[49], A. Ventura Barroso[49], R. Walsh[49], D. Wang[49], Q. Wang[49], K. Wichmann[49], L. Wiens[49,z], C. Wissing[49], Y. Yang[49], S. Zakharov[49], A. Zimermmane Castro Santos[49], A. Albrecht[50], A.R. Alves Andrade[50], M. Antonello[50], S. Bollweg[50], M. Bonanomi[50], K. El Morabit[50], Y. Fischer[50], M. Frahm[50], E. Garutti[50], A. Grohsjean[50], A.A. Guvenli[50], J. Haller[50], D. Hundhausen[50], G. Kasieczka[50], P. Keicher[50], R. Klanner[50], W. Korcari[50], T. Kramer[50], C.c. Kuo[50], F. Labe[50], J. Lange[50], A. Lobanov[50], L. Moureaux[50], M. Mrowietz[50], A. Nigamova[50], K. Nikolopoulos[50], Y. Nissan[50], A. Paasch[50], K.J. Pena Rodriguez[50], N. Prouvost[50], T. Quadfasel[50], B. Raciti[50], M. Rieger[50], D. Savoiu[50], P. Schleper[50], M. Schröder[50], J. Schwandt[50], M. Sommerhalder[50], H. Stadie[50], G. Steinbrück[50], A. Tews[50], R. Ward[50], B. Wiederspan[50], M. Wolf[50], S. Brommer[51], E. Butz[51], Y.M. Chen[51], T. Chwalek[51], A. Dierlamm[51], G.G. Dincer[51], U. Elicabuk[51], N. Faltermann[51], M. Giffels[51], A. Gottmann[51], F. Hartmann[51,ae], R. Hofsaess[51], M. Horzela[51], U. Husemann[51], J. Kieseler[51], M. Klute[51], R. Kunnilan Muhammed Rafeek[51], O. Lavoryk[51], J.M. Lawhorn[51], A. Lintuluoto[51], S. Maier[51], M. Mormile[51], Th. Müller[51], E. Pfeffer[51], M. Presilla[51], G. Quast[51], K. Rabbertz[51], B. Regnery[51], R. Schmieder[51], N. Shadskiy[51], I. Shvetsov[51], H.J. Simonis[51], L. Sowa[51], L. Stockmeier[51], K. Tauqeer[51], M. Toms[51], B. Topko[51], N. Trevisani[51], C. Verstege[51], T. Voigtländer[51], R.F. Von Cube[51], J. Von Den Driesch[51], M. Wassmer[51], R. Wolf[51], W.D. Zeuner[51], X. Zuo[51], G. Anagnostou[52], G. Daskalakis[52], A. Kyriakis[52], G. Melachroinos[53], Z. Painesis[53], I. Paraskevas[53], N. Saoulidou[53], K. Theofilatos[53], E. Tziaferi[53], E. Tzovara[53], K. Vellidis[53], I. Zisopoulos[53], T. Chatzistavrou[54], G. Karapostoli[54], K. Kousouris[54], E. Siamarkou[54], G. Tsipolitis[54], I. Bestintzanos[55], I. Evangelou[55], C. Foudas[55], P. Katsoulis[55], P. Kokkas[55], P.G. Kosmoglou Kioseoglou[55], N. Manthos[55], I. Papadopoulos[55], J. Strologas[55], D. Druzhkin[56], C. Hajdu[56], D. Horvath[56,af,ag], K. Márton[56], A.J. Rádl[56,ah], F. Sikler[56], V. Veszpremi[56], M. Csanád[57], K. Farkas[57], A. Fehérkuti[57,ai], M.M.A. Gadallah[57,aj], Á. Kadlecsik[57], M. León Coello[57], G. Pásztor[57], G.I. Veres[57], B. Ujvari[58], G. Zilizi[58], G. Bencze[59], S. Czellar[59], J. Molnar[59], Z. Szillasi[59], T. Csorgo[60,ai], F. Nemes[60,ai], T. Novak[60], I. Szanyi[60,ak], S. Bansal[61], S.B. Beri[61], V. Bhatnagar[61], G. Chaudhary[61], S. Chauhan[61], N. Dhingra[61,al], A. Kaur[61], A. Kaur[61], H. Kaur[61], M. Kaur[61], S. Kumar[61], T. Sheokand[61], J.B. Singh[61], A. Singla[61], A. Bhardwaj[62], A. Chhetri[62], B.C. Choudhary[62], A. Kumar[62], A. Kumar[62], M. Naimuddin[62], S. Phor[62], K. Ranjan[62], M.K. Saini[62], S. Acharya[63,am], B. Gomber[63,am], B. Sahu[63,am], S. Mukherjee[64], S. Baradia[65], S. Bhattacharya[65], S. Das Gupta[65], S. Dutta[65], S. Dutta[65], S. Sarkar[65], M.M. Ameen[66], P.K. Behera[66], S. Chatterjee[66], G. Dash[66], A. Dattamunsi[66], P. Jana[66], P. Kalbhor[66], S. Kamble[66], J.R. Komaragiri[66,an], T. Mishra[66], P.R. Pujahari[66], A.K. Sikdar[66], R.K. Singh[66], P. Verma[66], S. Verma[66], A. Vijay[66], B.K. Sirasva[67], L. Bhatt[68], S. Dugad[68], G.B. Mohanty[68], M. Shelake[68], P. Suryadevara[68], A. Bala[69], S. Banerjee[69], S. Barman[69,ao], R.M. Chatterjee[69], M. Guchait[69], Sh. Jain[69], A. Jaiswal[69], B.M. Joshi[69], S. Kumar[69], M. Maity[69,ao], G. Majumder[69], K. Mazumdar[69], S. Parolia[69], R. Saxena[69], A. Thachayath[69], S. Bahinipati[70,ap], D. Maity[70,aq], P. Mal[70], K. Naskar[70,aq], A. Nayak[70,aq], S. Nayak[70], K. Pal[70], R. Raturi[70], P. Sadangi[70], S.K. Swain[70],

JHEP03(2026)140

S. Varghese[70,aq], D. Vats[70,aq], A. Alpana[71], S. Dube[71], P. Hazarika[71], B. Kansal[71], A. Laha[71], R. Sharma[71], S. Sharma[71], K.Y. Vaish[71], S. Ghosh[72], H. Bakhshiansohi[73,ar], A. Jafari[73,as], V. Sedighzadeh Dalavi[73], M. Zeinali[73,at], S. Bashiri[74], S. Chenarani[74,au], S.M. Etesami[74], Y. Hosseini[74], M. Khakzad[74], E. Khazaie[74], M. Mohammadi Najafabadi[74], S. Tizchang[74,av], M. Felcini[75], M. Grunewald[75], M. Abbrescia[76a,76b], M. Barbieri[76a,76b], M. Buonsante[76a,76b], A. Colaleo[76a,76b], D. Creanza[76a,76c], B. D'Anzi[76a,76b], N. De Filippis[76a,76c], M. De Palma[76a,76b], W. Elmetenawee[76a,76b,q], N. Ferrara[76a,76c], L. Fiore[76a], L. Longo[76a], M. Louka[76a,76b], G. Maggi[76a,76c], M. Maggi[76a], I. Margjeka[76a], V. Mastrapasqua[76a,76b], S. My[76a,76b], F. Nenna[76a,76b], S. Nuzzo[76a,76b], A. Pellecchia[76a,76b], A. Pompili[76a,76b], G. Pugliese[76a,76c], R. Radogna[76a,76b], D. Ramos[76a], A. Ranieri[76a], L. Silvestris[76a], F.M. Simone[76a,76c], A. Stamerra[76a,76b], Ü. Sözbilir[76a], D. Troiano[76a,76b], R. Venditti[76a,76b], P. Verwilligen[76a], A. Zaza[76a,76b], C. Battilana[77a,77b], D. Bonacorsi[77a,77b], P. Capiluppi[77a,77b], F.R. Cavallo[77a], M. Cuffiani[77a,77b], G.M. Dallavalle[77a], T. Diotalevi[77a,77b], F. Fabbri[77a], A. Fanfani[77a,77b], D. Fasanella[77a], P. Giacomelli[77a], C. Grandi[77a], L. Guiducci[77a,77b], S. Lo Meo[77a,aw], M. Lorusso[77a,77b], L. Lunerti[77a], S. Marcellini[77a], G. Masetti[77a], F.L. Navarria[77a,77b], G. Paggi[77a,77b], A. Perrotta[77a], F. Primavera[77a,77b], A.M. Rossi[77a,77b], S. Rossi Tisbeni[77a,77b], T. Rovelli[77a,77b], G.P. Siroli[77a,77b], S. Costa[78a,78b,ax], A. Di Mattia[78a], A. Lapertosa[78a], R. Potenza[78a,78b], A. Tricomi[78a,78b,ax], J. Altork[79a,79b], P. Assiouras[79a], G. Barbagli[79a], G. Bardelli[79a], M. Bartolini[79a,79b], A. Calandri[79a,79b], B. Camaiani[79a,79b], A. Cassese[79a], R. Ceccarelli[79a], V. Ciulli[79a,79b], C. Civinini[79a], R. D'Alessandro[79a,79b], L. Damenti[79a,79b], E. Focardi[79a,79b], T. Kello[79a], G. Latino[79a,79b], P. Lenzi[79a,79b], M. Lizzo[79a], M. Meschini[79a], S. Paoletti[79a], A. Papanastassiou[79a,79b], G. Sguazzoni[79a], L. Viliani[79a], L. Benussi[80], S. Colafranceschi[80,ay], S. Meola[80,az], D. Piccolo[80], M. Alves Gallo Pereira[81a], F. Ferro[81a], E. Robutti[81a], S. Tosi[81a,81b], A. Benaglia[82a], F. Brivio[82a], V. Camagni[82a,82b], F. Cetorelli[82a,82b], F. De Guio[82a,82b], M.E. Dinardo[82a,82b], P. Dini[82a], S. Gennai[82a], R. Gerosa[82a,82b], A. Ghezzi[82a,82b], P. Govoni[82a,82b], L. Guzzi[82a], M.R. Kim[82a], G. Lavizzari[82a,82b], M.T. Lucchini[82a,82b], M. Malberti[82a], S. Malvezzi[82a], A. Massironi[82a], D. Menasce[82a], L. Moroni[82a], M. Paganoni[82a,82b], S. Palluotto[82a,82b], D. Pedrini[82a], A. Perego[82a,82b], B.S. Pinolini[82a], G. Pizzati[82a,82b], S. Ragazzi[82a,82b], T. Tabarelli de Fatis[82a,82b], S. Buontempo[83a], C. Di Fraia[83a,83b], F. Fabozzi[83a,83c], L. Favilla[83a,83d], A.O.M. Iorio[83a,83b], L. Lista[83a,83b,ba], P. Paolucci[83a,ae], B. Rossi[83a], P. Azzi[84a], N. Bacchetta[84a,bb], M. Biasotto[84a,bc], D. Bisello[84a,84b], P. Bortignon[84a,84c], G. Bortolato[84a,84b], A.C.M. Bulla[84a,84c], R. Carlin[84a,84b], T. Dorigo[84a,bd], F. Gasparini[84a,84b], S. Giorgetti[84a], E. Lusiani[84a], M. Margoni[84a,84b], A.T. Meneguzzo[84a,84b], J. Pazzini[84a,84b], P. Ronchese[84a,84b], R. Rossin[84a,84b], F. Simonetto[84a,84b], M. Tosi[84a,84b], A. Triossi[84a,84b], S. Ventura[84a], M. Zanetti[84a,84b], P. Zotto[84a,84b], A. Zucchetta[84a,84b], G. Zumerle[84a,84b], A. Braghieri[85a], S. Calzaferri[85a], P. Montagna[85a,85b], M. Pelliccioni[85a], V. Re[85a], C. Riccardi[85a,85b], P. Salvini[85a], I. Vai[85a,85b], P. Vitulo[85a,85b], S. Ajmal[86a,86b], M.E. Ascioti[86a,86b], G.M. Bilei[86a], C. Carrivale[86a,86b], D. Ciangottini[86a,86b], L. Della Penna[86a,86b], L. Fanò[86a,86b], V. Mariani[86a,86b], M. Menichelli[86a], F. Moscatelli[86a,be], A. Rossi[86a,86b], A. Santocchia[86a,86b], D. Spiga[86a], T. Tedeschi[86a,86b], C. Aimè[87a,87b], C.A. Alexe[87a,87c], P. Asenov[87a,87b], P. Azzurri[87a], G. Bagliesi[87a], R. Bhattacharya[87a],

JHEP03(2026)140

L. Bianchini[87a,87b], T. Boccali[87a], E. Bossini[87a], D. Bruschini[87a,87c], L. Calligaris[87a,87b], R. Castaldi[87a], F. Cattafesta[87a,87c], M.A. Ciocci[87a,87d], M. Cipriani[87a,87b], R. Dell'Orso[87a], S. Donato[87a,87b], R. Forti[87a,87b], A. Giassi[87a], F. Ligabue[87a,87c], A.C. Marini[87a,87b], D. Matos Figueiredo[87a], A. Messineo[87a,87b], S. Mishra[87a], V.K. Muraleedharan Nair Bindhu[87a,87b], S. Nandan[87a], F. Palla[87a], M. Riggirello[87a,87c], A. Rizzi[87a,87b], G. Rolandi[87a,87c], S. Roy Chowdhury[87a,bf], T. Sarkar[87a], A. Scribano[87a], P. Solanki[87a,87b], P. Spagnolo[87a], F. Tenchini[87a,87b], R. Tenchini[87a], G. Tonelli[87a,87b], N. Turini[87a,87d], F. Vaselli[87a,87c], A. Venturi[87a], P.G. Verdini[87a], P. Akrap[88a,88b], C. Basile[88a,88b], S.C. Behera[88a], F. Cavallari[88a], L. Cunqueiro Mendez[88a,88b], F. De Riggi[88a,88b], D. Del Re[88a,88b], E. Di Marco[88a], M. Diemoz[88a], F. Errico[88a], L. Frosina[88a,88b], R. Gargiulo[88a,88b], B. Harikrishnan[88a,88b], F. Lombardi[88a,88b], E. Longo[88a,88b], L. Martikainen[88a,88b], J. Mijuskovic[88a,88b], G. Organtini[88a,88b], N. Palmeri[88a,88b], R. Paramatti[88a,88b], C. Quaranta[88a,88b], S. Rahatlou[88a,88b], C. Rovelli[88a], F. Santanastasio[88a,88b], L. Soffi[88a], V. Vladimirov[88a,88b], N. Amapane[89a,89b], R. Arcidiacono[89a,89c], S. Argiro[89a,89b], M. Arneodo[89a,89c], N. Bartosik[89a,89c], R. Bellan[89a,89b], A. Bellora[89a,89b], C. Biino[89a], C. Borca[89a,89b], N. Cartiglia[89a], M. Costa[89a,89b], R. Covarelli[89a,89b], N. Demaria[89a], L. Finco[89a], M. Grippo[89a,89b], B. Kiani[89a,89b], L. Lanteri[89a,89b], F. Legger[89a], F. Luongo[89a,89b], C. Mariotti[89a], S. Maselli[89a], A. Mecca[89a,89b], L. Menzio[89a,89b], P. Meridiani[89a], E. Migliore[89a,89b], M. Monteno[89a], M.M. Obertino[89a,89b], G. Ortona[89a], L. Pacher[89a,89b], N. Pastrone[89a], M. Ruspa[89a,89c], F. Siviero[89a,89b], V. Sola[89a,89b], A. Solano[89a,89b], A. Staiano[89a], C. Tarricone[89a,89b], D. Trocino[89a], G. Umoret[89a,89b], E. Vlasov[89a,89b], R. White[89a,89b], J. Babbar[90a,90b], S. Belforte[90a], V. Candelise[90a,90b], M. Casarsa[90a], F. Cossutti[90a], K. De Leo[90a], G. Della Ricca[90a,90b], R. Delli Gatti[90a,90b], S. Dogra[91], J. Hong[91], J. Kim[91], T. Kim[91], D. Lee[91], H. Lee[91], J. Lee[91], S.W. Lee[91], C.S. Moon[91], Y.D. Oh[91], S. Sekmen[91], B. Tae[91], Y.C. Yang[91], M.S. Kim[92], G. Bak[93], P. Gwak[93], H. Kim[93], D.H. Moon[93], J. Seo[93], E. Asilar[94], F. Carnevali[94], J. Choi[94,bg], T.J. Kim[94], Y. Ryou[94], S. Ha[95], S. Han[95], B. Hong[95], J. Kim[95], K. Lee[95], K.S. Lee[95], S. Lee[95], J. Yoo[95], J. Goh[96], J. Shin[96], S. Yang[96], Y. Kang[97], H. S. Kim[97], Y. Kim[97], S. Lee[97], J. Almond[98], J.H. Bhyun[98], J. Choi[98], J. Choi[98], W. Jun[98], H. Kim[98], J. Kim[98], T. Kim[98], Y. Kim[98], Y.W. Kim[98], S. Ko[98], H. Lee[98], J. Lee[98], J. Lee[98], B.H. Oh[98], S.B. Oh[98], J. Shin[98], U.K. Yang[98], I. Yoon[98], W. Jang[99], D.Y. Kang[99], D. Kim[99], S. Kim[99], B. Ko[99], J.S.H. Lee[99], Y. Lee[99], I.C. Park[99], Y. Roh[99], I.J. Watson[99], G. Cho[100], K. Hwang[100], B. Kim[100], S. Kim[100], K. Lee[100], H.D. Yoo[100], M. Choi[101], Y. Lee[101], I. Yu[101], T. Beyrouthy[102], Y. Gharbia[102], F. Alazemi[103], K. Dreimanis[104], O.M. Eberlins[104], A. Gaile[104], C. Munoz Diaz[104], D. Osite[104], G. Pikurs[104], R. Plese[104], A. Potrebko[104], M. Seidel[104], D. Sidiropoulos Kontos[104], N.R. Strautnieks[105], M. Ambrozas[106], A. Juodagalvis[106], S. Nargelas[106], A. Rinkevicius[106], G. Tamulaitis[106], I. Yusuff[107,bh], Z. Zolkapli[107], J.F. Benitez[108], A. Castaneda Hernandez[108], A. Cota Rodriguez[108], L.E. Cuevas Picos[108], H.A. Encinas Acosta[108], L.G. Gallegos Maríñez[108], J.A. Murillo Quijada[108], A. Sehrawat[108], L. Valencia Palomo[108], G. Ayala[109], H. Castilla-Valdez[109], H. Crotte Ledesma[109], R. Lopez-Fernandez[109], J. Mejia Guisao[109], R. Reyes-Almanza[109], A. Sánchez Hernández[109], C. Oropeza Barrera[110], D.L. Ramirez Guadarrama[110],

JHEP03(2026)140

M. Ramírez García[110], I. Bautista[111], F.E. Neri Huerta[111], I. Pedraza[111], H.A. Salazar Ibarguen[111], C. Uribe Estrada[111], I. Bubanja[112], N. Raicevic[112], P.H. Butler[113], A. Ahmad[114], M.I. Asghar[114], A. Awais[114], M.I.M. Awan[114], W.A. Khan[114], V. Avati[115], L. Forthomme[115], L. Grzanka[115], M. Malawski[115], K. Piotrzkowski[115], M. Bluj[116], M. Górski[116], M. Kazana[116], M. Szleper[116], P. Zalewski[116], K. Bunkowski[117], K. Doroba[117], A. Kalinowski[117], M. Konecki[117], J. Krolikowski[117], A. Muhammad[117], P. Fokow[118], K. Pozniak[118], W. Zabolotny[118], M. Araujo[119], D. Bastos[119], C. Beirão Da Cruz E Silva[119], A. Boletti[119], M. Bozzo[119], T. Camporesi[119], G. Da Molin[119], M. Gallinaro[119], J. Hollar[119], N. Leonardo[119], G.B. Marozzo[119], A. Petrilli[119], M. Pisano[119], J. Seixas[119], J. Varela[119], J.W. Wulff[119], P. Adzic[120], L. Markovic[120], P. Milenovic[120], V. Milosevic[120], D. Devetak[121], M. Dordevic[121], J. Milosevic[121], L. Nadderd[121], V. Rekovic[121], M. Stojanovic[121], M. Alcalde Martinez[122], J. Alcaraz Maestre[122], J.A. Brochero Cifuentes[122], M. Cepeda[122], M. Cerrada[122], N. Colino[122], J. Cuchillo Ortega[122], B. De La Cruz[122], A. Delgado Peris[122], A. Escalante Del Valle[122], Cristina F. Bedoya[122], D. Fernández Del Val[122], J.P. Fernández Ramos[122], J. Flix[122], M.C. Fouz[122], M. Gonzalez Hernandez[122], O. Gonzalez Lopez[122], S. Goy Lopez[122], J.M. Hernandez[122], M.I. Josa[122], J. Llorente Merino[122], Oliver M. Carretero[122], C. Martin Perez[122], E. Martin Viscasillas[122], D. Moran[122], C. M. Morcillo Perez[122], R. Paz Herrera[122], C. Perez Dengra[122], J. Puerta Pelayo[122], A. Pérez-Calero Yzquierdo[122], I. Redondo[122], J. Vazquez Escobar[122], J.F. de Trocóniz[123], B. Alvarez Gonzalez[124], J. Ayllon Torresano[124], A. Cardini[124], J. Cuevas[124], J. Del Riego Badas[124], D. Estrada Acevedo[124], J. Fernandez Menendez[124], S. Folgueras[124], I. Gonzalez Caballero[124], P. Leguina[124], M. Obeso Menendez[124], E. Palencia Cortezon[124], J. Prado Pico[124], A. Soto Rodríguez[124], C. Vico Villalba[124], P. Vischia[124], S. Blanco Fernández[125], I.J. Cabrillo[125], A. Calderon[125], J. Duarte Campderros[125], M. Fernandez[125], G. Gomez[125], C. Lasaosa García[125], R. Lopez Ruiz[125], C. Martinez Rivero[125], P. Martinez Ruiz del Arbol[125], F. Matorras[125], P. Matorras Cuevas[125], E. Navarrete Ramos[125], J. Piedra Gomez[125], C. Quintana San Emeterio[125], L. Scodellaro[125], I. Vila[125], R. Vilar Cortabitarte[125], J.M. Vizan Garcia[125], D.D.C. Wickramarathna[126], B. Kailasapathy[126,bi], W.G.D. Dharmaratna[127,bj], K. Liyanage[127], N. Perera[127], D. Abbaneo[128], C. Amendola[128], R. Ardino[128], E. Auffray[128], J. Baechler[128], D. Barney[128], M. Bianco[128], A. Bocci[128], L. Borgonovi[128], C. Botta[128], A. Bragagnolo[128], C.E. Brown[128], C. Caillol[128], G. Cerminara[128], P. Connor[128], D. d'Enterria[128], A. Dabrowski[128], A. David[128], A. De Roeck[128], M.M. Defranchis[128], M. Deile[128], M. Dobson[128], P.J. Fernández Manteca[128], W. Funk[128], A. Gaddi[128], S. Giani[128], D. Gigi[128], K. Gill[128], F. Glege[128], M. Glowacki[128], A. Gruber[128], J. Hegeman[128], J.K. Heikkilä[128], B. Huber[128], V. Innocente[128], T. James[128], P. Janot[128], O. Kaluzinska[128], O. Karacheban[128,ab], G. Karathanasis[128], S. Laurila[128], P. Lecoq[128], C. Lourenço[128], A.-M. Lyon[128], M. Magherini[128], L. Malgeri[128], M. Mannelli[128], A. Mehta[128], F. Meijers[128], J.A. Merlin[128], S. Mersi[128], E. Meschi[128], M. Migliorini[128], F. Monti[128], F. Moortgat[128], M. Mulders[128], M. Musich[128], I. Neutelings[128], S. Orfanelli[128], F. Pantaleo[128], M. Pari[128], G. Petrucciani[128], A. Pfeiffer[128], M. Pierini[128], M. Pitt[128], H. Qu[128], D. Rabady[128],

JHEP03(2026)140

A. Reimers[128], B. Ribeiro Lopes[128], F. Riti[128], P. Rosado[128], M. Rovere[128], H. Sakulin[128], R. Salvatico[128], S. Sanchez Cruz[128], S. Scarfi[128], M. Selvaggi[128], A. Sharma[128], K. Shchelina[128], P. Silva[128], P. Sphicas[128,bk], A.G. Stahl Leiton[128], A. Steen[128], S. Summers[128], D. Treille[128], P. Tropea[128], E. Vernazza[128], J. Wanczyk[128,bl], J. Wang[128], S. Wuchterl[128], M. Zarucki[128], P. Zehetner[128], P. Zejdl[128], G. Zevi Della Porta[128], T. Bevilacqua[129,bm], L. Caminada[129,bm], W. Erdmann[129], R. Horisberger[129], Q. Ingram[129], H.C. Kaestli[129], D. Kotlinski[129], C. Lange[129], U. Langenegger[129], L. Noehte[129,bm], T. Rohe[129], A. Samalan[129], T.K. Aarrestad[130], M. Backhaus[130], G. Bonomelli[130], C. Cazzaniga[130], K. Datta[130], P. De Bryas Dexmiers D'archiacchiac[130,bl], A. De Cosa[130], G. Dissertori[130], M. Dittmar[130], M. Donegà[130], F. Eble[130], K. Gedia[130], F. Glessgen[130], C. Grab[130], T.G. Harte[130], N. Härringer[130], W. Lustermann[130], M. Malucchi[130], R.A. Manzoni[130], M. Marchegiani[130], L. Marchese[130], A. Mascellani[130,bl], F. Nessi-Tedaldi[130], F. Pauss[130], V. Perovic[130], B. Ristic[130], R. Seidita[130], J. Steggemann[130,bl], A. Tarabini[130], D. Valsecchi[130], R. Wallny[130], C. Amsler[131,bn], F. Bilandzija[131], P. Bärtschi[131], M.F. Canelli[131], G. Celotto[131], K. Cormier[131], M. Huwiler[131], W. Jin[131], A. Jofrehei[131], B. Kilminster[131], T.H. Kwok[131], S. Leontsinis[131], V. Lukashenko[131], A. Macchiolo[131], F. Meng[131], M. Missiroli[131], J. Motta[131], P. Robmann[131], M. Senger[131], E. Shokr[131], F. Stäger[131], R. Tramontano[131], D. Bhowmik[132], C.M. Kuo[132], P.K. Rout[132], S. Taj[132], P.C. Tiwari[132,an], L. Ceard[133], K.F. Chen[133], Z.g. Chen[133], A. De Iorio[133], W.-S. Hou[133], T.h. Hsu[133], Y.w. Kao[133], S. Karmakar[133], G. Kole[133], Y.y. Li[133], R.-S. Lu[133], E. Paganis[133], X.f. Su[133], J. Thomas-Wilsker[133], L.s. Tsai[133], D. Tsionou[133], H.y. Wu[133], E. Yazgan[133], C. Asawatangtrakuldee[134], N. Srimanobhas[134], Y. Maghrbi[135], D. Agyel[136], F. Dolek[136], I. Dumanoglu[136,bo], Y. Guler[136,bp], E. Gurpinar Guler[136,bp], C. Isik[136], O. Kara[136], A. Kayis Topaksu[136], Y. Komurcu[136], G. Onengut[136], K. Ozdemir[136,bq], B. Tali[136,br], U.G. Tok[136], E. Uslan[136], I.S. Zorbakir[136], M. Yalvac[137,bs], B. Akgun[138], I.O. Atakisi[138,bt], E. Gülmez[138], M. Kaya[138,bu], O. Kaya[138,bv], M.A. Sarkisla[138,bw], S. Tekten[138,bx], A. Cakir[139], K. Cankocak[139,bo,by], S. Sen[139,bz], O. Aydilek[140,ca], B. Hacisahinoglu[140], I. Hos[140,cb], B. Kaynak[140], S. Ozkorucuklu[140], O. Potok[140], H. Sert[140], C. Simsek[140], C. Zorbilmez[140], S. Cerci[141], B. Isildak[141,cc], E. Simsek[141], D. Sunar Cerci[141], T. Yetkin[141,w], A. Boyaryntsev[142], O. Dadazhanova[142], B. Grynyov[142], L. Levchuk[143], J.J. Brooke[144], A. Bundock[144], F. Bury[144], E. Clement[144], D. Cussans[144], D. Dharmender[144], H. Flacher[144], J. Goldstein[144], H.F. Heath[144], M.-L. Holmberg[144], L. Kreczko[144], S. Paramesvaran[144], L. Robertshaw[144], M.S. Sanjrani[144,ar], J. Segal[144], V.J. Smith[144], A.H. Ball[145], K.W. Bell[145], A. Belyaev[145,cd], C. Brew[145], R.M. Brown[145], D.J.A. Cockerill[145], A. Elliot[145], K.V. Ellis[145], J. Gajownik[145], K. Harder[145], S. Harper[145], J. Linacre[145], K. Manolopoulos[145], M. Moallemi[145], D.M. Newbold[145], E. Olaiya[145], D. Petyt[145], T. Reis[145], A.R. Sahasransu[145], G. Salvi[145], T. Schuh[145], C.H. Shepherd-Themistocleous[145], I.R. Tomalin[145], K.C. Whalen[145], T. Williams[145], I. Andreou[146], R. Bainbridge[146], P. Bloch[146], O. Buchmuller[146], C.A. Carrillo Montoya[146], D. Colling[146], J.S. Dancu[146], I. Das[146], P. Dauncey[146], G. Davies[146], M. Della Negra[146], S. Fayer[146], G. Fedi[146], G. Hall[146], H.R. Hoorani[146], A. Howard[146], G. Iles[146], C.R. Knight[146], P. Krueper[146], J. Langford[146], K.H. Law[146], E. Leutgeb[146],

JHEP03(2026)140

J. León Holgado[146], L. Lyons[146], A.-M. Magnan[146], B. Maier[146], S. Mallios[146], A. Mastronikolis[146], M. Mieskolainen[146], J. Nash[146,ce], M. Pesaresi[146], P.B. Pradeep[146], B.C. Radburn-Smith[146], A. Richards[146], A. Rose[146], L. Russell[146], K. Savva[146], C. Seez[146], R. Shukla[146], A. Tapper[146], K. Uchida[146], G.P. Uttley[146], T. Virdee[146,ae], M. Vojinovic[146], N. Wardle[146], D. Winterbottom[146], J.E. Cole[147], A. Khan[147], P. Kyberd[147], I.D. Reid[147], S. Abdullin[148], A. Brinkerhoff[148], E. Collins[148], M.R. Darwish[148], J. Dittmann[148], K. Hatakeyama[148], V. Hegde[148], J. Hiltbrand[148], B. McMaster[148], J. Samudio[148], S. Sawant[148], C. Sutantawibul[148], J. Wilson[148], J.M. Hogan[149,cf], R. Bartek[150], A. Dominguez[150], S. Raj[150], A.E. Simsek[150], S.S. Yu[150], B. Bam[151], A. Buchot Perraguin[151], S. Campbell[151], R. Chudasama[151], S.I. Cooper[151], C. Crovella[151], G. Fidalgo[151], S.V. Gleyzer[151], A. Khukhunaishvili[151], K. Matchev[151], E. Pearson[151], C.U. Perez[151], P. Rumerio[151,cg], E. Usai[151], R. Yi[151], S. Cholak[152], G. De Castro[152], Z. Demiragli[152], C. Erice[152], C. Fangmeier[152], C. Fernandez Madrazo[152], E. Fontanesi[152], J. Fulcher[152], F. Golf[152], S. Jeon[152], J. O'Cain[152], I. Reed[152], J. Rohlf[152], K. Salyer[152], D. Sperka[152], D. Spitzbart[152], I. Suarez[152], A. Tsatsos[152], E. Wurtz[152], A.G. Zecchinelli[152], G. Barone[153], G. Benelli[153], D. Cutts[153], S. Ellis[153], L. Gouskos[153], M. Hadley[153], U. Heintz[153], K.W. Ho[153], T. Kwon[153], G. Landsberg[153], K.T. Lau[153], J. Luo[153], S. Mondal[153], J. Roloff[153], T. Russell[153], S. Sagir[153,ch], X. Shen[153], M. Stamenkovic[153], N. Venkatasubramanian[153], S. Abbott[154], B. Barton[154], R. Breedon[154], H. Cai[154], M. Calderon De La Barca Sanchez[154], M. Chertok[154], M. Citron[154], J. Conway[154], P.T. Cox[154], R. Erbacher[154], O. Kukral[154], G. Mocellin[154], S. Ostrom[154], I. Salazar Segovia[154], W. Wei[154], S. Yoo[154], K. Adamidis[155], M. Bachtis[155], D. Campos[155], R. Cousins[155], A. Datta[155], G. Flores Avila[155], J. Hauser[155], M. Ignatenko[155], M.A. Iqbal[155], T. Lam[155], Y.f. Lo[155], E. Manca[155], A. Nunez Del Prado[155], D. Saltzberg[155], V. Valuev[155], R. Clare[156], J.W. Gary[156], G. Hanson[156], A. Aportela[157], A. Arora[157], J.G. Branson[157], S. Cittolin[157], S. Cooperstein[157], D. Diaz[157], J. Duarte[157], L. Giannini[157], Y. Gu[157], J. Guiang[157], V. Krutelyov[157], R. Lee[157], J. Letts[157], H. Li[157], M. Masciovecchio[157], F. Mokhtar[157], S. Mukherjee[157], M. Pieri[157], D. Primosch[157], M. Quinnan[157], V. Sharma[157], M. Tadel[157], E. Vourliotis[157], F. Würthwein[157], A. Yagil[157], Z. Zhao[157], A. Barzdukas[158], L. Brennan[158], C. Campagnari[158], S. Carron Montero[158,ci], K. Downham[158], C. Grieco[158], M.M. Hussain[158], J. Incandela[158], M.W.K. Lai[158], A.J. Li[158], P. Masterson[158], J. Richman[158], S.N. Santpur[158], U. Sarica[158], R. Schmitz[158], F. Setti[158], J. Sheplock[158], D. Stuart[158], T.Á. Vámi[158], X. Yan[158], D. Zhang[158], A. Albert[159], S. Bhattacharya[159], A. Bornheim[159], O. Cerri[159], R. Kansal[159], J. Mao[159], H.B. Newman[159], G. Reales Gutiérrez[159], T. Sievert[159], M. Spiropulu[159], J.R. Vlimant[159], R.A. Wynne[159], S. Xie[159], J. Alison[160], S. An[160], M. Cremonesi[160], V. Dutta[160], E.Y. Ertorer[160], T. Ferguson[160], T.A. Gómez Espinosa[160], A. Harilal[160], A. Kallil Tharayil[160], M. Kanemura[160], C. Liu[160], P. Meiring[160], T. Mudholkar[160], S. Murthy[160], P. Palit[160], K. Park[160], M. Paulini[160], A. Roberts[160], A. Sanchez[160], W. Terrill[160], J.P. Cumalat[161], W.T. Ford[161], A. Hart[161], A. Hassani[161], S. Kwan[161], J. Pearkes[161], C. Savard[161], N. Schonbeck[161], K. Stenson[161], K.A. Ulmer[161], S.R. Wagner[161], N. Zipper[161], D. Zuolo[161], J. Alexander[162], X. Chen[162], D.J. Cranshaw[162], J. Dickinson[162],

JHEP03(2026)140

A. Duquette[162], J. Fan[162], X. Fan[162], J. Grassi[162], S. Hogan[162], P. Kotamnives[162], J. Monroy[162], G. Niendorf[162], M. Oshiro[162], J.R. Patterson[162], M. Reid[162], A. Ryd[162], J. Thom[162], P. Wittich[162], R. Zou[162], L. Zygala[162], M. Albrow[163], M. Alyari[163], O. Amram[163], G. Apollinari[163], A. Apresyan[163], L.A.T. Bauerdick[163], D. Berry[163], J. Berryhill[163], P.C. Bhat[163], K. Burkett[163], J.N. Butler[163], A. Canepa[163], G.B. Cerati[163], H.W.K. Cheung[163], F. Chlebana[163], C. Cosby[163], G. Cummings[163], I. Dutta[163], V.D. Elvira[163], J. Freeman[163], A. Gandrakota[163], Z. Gecse[163], L. Gray[163], D. Green[163], A. Grummer[163], S. Grünendahl[163], D. Guerrero[163], O. Gutsche[163], R.M. Harris[163], T.C. Herwig[163], J. Hirschauer[163], B. Jayatilaka[163], S. Jindariani[163], M. Johnson[163], U. Joshi[163], T. Klijnsma[163], B. Klima[163], K.H.M. Kwok[163], S. Lammel[163], C. Lee[163], D. Lincoln[163], R. Lipton[163], T. Liu[163], K. Maeshima[163], D. Mason[163], P. McBride[163], P. Merkel[163], S. Mrenna[163], S. Nahn[163], J. Ngadiuba[163], D. Noonan[163], S. Norberg[163], V. Papadimitriou[163], N. Pastika[163], K. Pedro[163], C. Pena[163,cj], C.E. Perez Lara[163], F. Ravera[163], A. Reinsvold Hall[163,ck], L. Ristori[163], M. Safdari[163], E. Sexton-Kennedy[163], N. Smith[163], A. Soha[163], L. Spiegel[163], S. Stoynev[163], J. Strait[163], L. Taylor[163], S. Tkaczyk[163], N.V. Tran[163], L. Uplegger[163], E.W. Vaandering[163], C. Wang[163], I. Zoi[163], C. Aruta[164], P. Avery[164], D. Bourilkov[164], P. Chang[164], V. Cherepanov[164], R.D. Field[164], C. Huh[164], E. Koenig[164], M. Kolosova[164], J. Konigsberg[164], A. Korytov[164], N. Menendez[164], G. Mitselmakher[164], K. Mohrman[164], A. Muthirakalayil Madhu[164], N. Rawal[164], S. Rosenzweig[164], V. Sulimov[164], Y. Takahashi[164], J. Wang[164], T. Adams[165], A. Al Kadhim[165], A. Askew[165], S. Bower[165], R. Goff[165], R. Hashmi[165], R.S. Kim[165], T. Kolberg[165], G. Martinez[165], M. Mazza[165], H. Prosper[165], P.R. Prova[165], M. Wulansatiti[165], R. Yohay[165], B. Alsufyani[166], S. Butalla[166], S. Das[166], M. Hohlmann[166], M. Lavinsky[166], E. Yanes[166], M.R. Adams[167], N. Barnett[167], A. Baty[167], C. Bennett[167], R. Cavanaugh[167], D. S. Lemos[167], R. Escobar Franco[167], O. Evdokimov[167], C.E. Gerber[167], H. Gupta[167], M. Hawksworth[167], A. Hingrajiya[167], D.J. Hofman[167], J.h. Lee[167], C. Mills[167], S. Nanda[167], G. Nigmatkulov[167], B. Ozek[167], T. Phan[167], D. Pilipovic[167], R. Pradhan[167], E. Prifti[167], P. Roy[167], T. Roy[167], N. Singh[167], M.B. Tonjes[167], N. Varelas[167], M.A. Wadud[167], J. Yoo[167], M. Alhusseini[168], D. Blend[168], K. Dilsiz[168,cl], O.K. Köseyan[168], A. Mestvirishvili[168,cm], O. Neogi[168], H. Ogul[168,cn], Y. Onel[168], A. Penzo[168], C. Snyder[168], E. Tiras[168,co], B. Blumenfeld[169], J. Davis[169], A.V. Gritsan[169], L. Kang[169], S. Kyriacou[169], P. Maksimovic[169], M. Roguljic[169], S. Sekhar[169], M.V. Srivastav[169], M. Swartz[169], A. Abreu[170], L.F. Alcerro Alcerro[170], J. Anguiano[170], S. Arteaga Escatel[170], P. Baringer[170], A. Bean[170], Z. Flowers[170], D. Grove[170], J. King[170], G. Krintiras[170], M. Lazarovits[170], C. Le Mahieu[170], J. Marquez[170], M. Murray[170], M. Nickel[170], S. Popescu[170,cp], C. Rogan[170], C. Royon[170], S. Rudrabhatla[170], S. Sanders[170], C. Smith[170], G. Wilson[170], B. Allmond[171], N. Islam[171], A. Ivanov[171], K. Kaadze[171], Y. Maravin[171], J. Natoli[171], G.G. Reddy[171], D. Roy[171], G. Sorrentino[171], A. Baden[172], A. Belloni[172], J. Bistany-riebman[172], S.C. Eno[172], N.J. Hadley[172], S. Jabeen[172], R.G. Kellogg[172], T. Koeth[172], B. Kronheim[172], S. Lascio[172], P. Major[172], A.C. Mignerey[172], C. Palmer[172], C. Papageorgakis[172], M.M. Paranjpe[172], E. Popova[172,cq], A. Shevelev[172], L. Zhang[172], C. Baldenegro Barrera[173], J. Bendavid[173], H. Bossi[173],

JHEP03(2026)140

S. Bright-Thonney[173], I.A. Cali[173], Y.c. Chen[173], P.c. Chou[173], M. D'Alfonso[173], J. Eysermans[173], C. Freer[173], G. Gomez-Ceballos[173], M. Goncharov[173], G. Grosso[173], P. Harris[173], D. Hoang[173], G.M. Innocenti[173], D. Kovalskyi[173], J. Krupa[173], L. Lavezzo[173], Y.-J. Lee[173], K. Long[173], C. Mcginn[173], A. Novak[173], M.I. Park[173], C. Paus[173], C. Reissel[173], C. Roland[173], G. Roland[173], S. Rothman[173], T.a. Sheng[173], G.S.F. Stephans[173], D. Walter[173], Z. Wang[173], B. Wyslouch[173], T. J. Yang[173], B. Crossman[174], W.J. Jackson[174], C. Kapsiak[174], M. Krohn[174], D. Mahon[174], J. Mans[174], B. Marzocchi[174], R. Rusack[174], O. Sancar[174], R. Saradhy[174], N. Strobbe[174], K. Bloom[175], D.R. Claes[175], G. Haza[175], J. Hossain[175], C. Joo[175], I. Kravchenko[175], A. Rohilla[175], J.E. Siado[175], W. Tabb[175], A. Vagnerini[175], A. Wightman[175], F. Yan[175], H. Bandyopadhyay[176], L. Hay[176], H.w. Hsia[176], I. Iashvili[176], A. Kalogeropoulos[176], A. Kharchilava[176], A. Mandal[176], M. Morris[176], D. Nguyen[176], S. Rappoccio[176], H. Rejeb Sfar[176], A. Williams[176], P. Young[176], D. Yu[176], G. Alverson[177], E. Barberis[177], J. Bonilla[177], B. Bylsma[177], M. Campana[177], J. Dervan[177], Y. Haddad[177], Y. Han[177], I. Israr[177], A. Krishna[177], M. Lu[177], N. Manganelli[177], R. Mccarthy[177], D.M. Morse[177], T. Orimoto[177], A. Parker[177], L. Skinnari[177], C.S. Thoreson[177], E. Tsai[177], D. Wood[177], S. Dittmer[178], K.A. Hahn[178], Y. Liu[178], M. Mcginnis[178], Y. Miao[178], D.G. Monk[178], M.H. Schmitt[178], A. Taliercio[178], M. Velasco[178], J. Wang[178], G. Agarwal[179], R. Band[179], R. Bucci[179], S. Castells[179], A. Das[179], A. Ehnis[179], R. Goldouzian[179], M. Hildreth[179], K. Hurtado Anampa[179], T. Ivanov[179], C. Jessop[179], A. Karneyeu[179], K. Lannon[179], J. Lawrence[179], N. Loukas[179], L. Lutton[179], J. Mariano[179], N. Marinelli[179], I. Mcalister[179], T. McCauley[179], C. Mcgrady[179], C. Moore[179], Y. Musienko[179,cr], H. Nelson[179], M. Osherson[179], A. Piccinelli[179], R. Ruchti[179], A. Townsend[179], Y. Wan[179], M. Wayne[179], H. Yockey[179], A. Basnet[180], M. Carrigan[180], R. De Los Santos[180], L.S. Durkin[180], C. Hill[180], M. Joyce[180], M. Nunez Ornelas[180], D.A. Wenzl[180], B.L. Winer[180], B. R. Yates[180], H. Bouchamaoui[181], K. Coldham[181], P. Das[181], G. Dezoort[181], P. Elmer[181], A. Frankenthal[181], M. Galli[181], B. Greenberg[181], N. Haubrich[181], K. Kennedy[181], G. Kopp[181], Y. Lai[181], D. Lange[181], A. Loeliger[181], D. Marlow[181], I. Ojalvo[181], J. Olsen[181], F. Simpson[181], D. Stickland[181], C. Tully[181], S. Malik[182], R. Sharma[182], S. Chandra[183], R. Chawla[183], A. Gu[183], L. Gutay[183], M. Jones[183], A.W. Jung[183], D. Kondratyev[183], M. Liu[183], G. Negro[183], N. Neumeister[183], G. Paspalaki[183], S. Piperov[183], N.R. Saha[183], J.F. Schulte[183], F. Wang[183], A. Wildridge[183], W. Xie[183], Y. Yao[183], Y. Zhong[183], N. Parashar[184], A. Pathak[184], E. Shumka[184], D. Acosta[185], A. Agrawal[185], C. Arbour[185], T. Carnahan[185], K.M. Ecklund[185], S. Freed[185], P. Gardner[185], F.J.M. Geurts[185], T. Huang[185], I. Krommydas[185], N. Lewis[185], W. Li[185], J. Lin[185], O. Miguel Colin[185], B.P. Padley[185], R. Redjimi[185], J. Rotter[185], E. Yigitbasi[185], Y. Zhang[185], O. Bessidskaia Bylund[186], A. Bodek[186], P. de Barbaro[186,†], R. Demina[186], A. Garcia-Bellido[186], H.S. Hare[186], O. Hindrichs[186], N. Parmar[186], P. Parygin[186,cq], H. Seo[186], R. Taus[186], B. Chiarito[187], J.P. Chou[187], S.V. Clark[187], S. Donnelly[187], D. Gadkari[187], Y. Gershtein[187], E. Halkiadakis[187], C. Houghton[187], D. Jaroslawski[187], A. Kobert[187], S. Konstantinou[187], I. Laflotte[187], A. Lath[187], J. Martins[187], M. Heindl[187], B. Rand[187], J. Reichert[187], P. Saha[187], S. Salur[187], S. Schnetzer[187], S. Somalwar[187], R. Stone[187], S.A. Thayil[187],

JHEP03(2026)140

S. Thomas[187], J. Vora[187], D. Ally[188], A.G. Delannoy[188], S. Fiorendi[188], J. Harris[188], S. Higginbotham[188], T. Holmes[188], A.R. Kanuganti[188], N. Karunarathna[188], J. Lawless[188], L. Lee[188], E. Nibigira[188], B. Skipworth[188], S. Spanier[188], D. Aebi[189], M. Ahmad[189], T. Akhter[189], K. Androsov[189], A. Bolshov[189], O. Bouhali[189,cs], A. Cagnotta[189], V. D'Amante[189], R. Eusebi[189], P. Flanagan[189], J. Gilmore[189], Y. Guo[189], T. Kamon[189], S. Luo[189], R. Mueller[189], A. Safonov[189], N. Akchurin[190], J. Damgov[190], Y. Feng[190], N. Gogate[190], Y. Kazhykarim[190], K. Lamichhane[190], S.W. Lee[190], C. Madrid[190], A. Mankel[190], T. Peltola[190], I. Volobouev[190], E. Appelt[191], Y. Chen[191], S. Greene[191], A. Gurrola[191], W. Johns[191], R. Kunnawalkam Elayavalli[191], A. Melo[191], D. Rathjens[191], F. Romeo[191], P. Sheldon[191], S. Tuo[191], J. Velkovska[191], J. Viinikainen[191], J. Zhang[191], B. Cardwell[192], H. Chung[192], B. Cox[192], J. Hakala[192], R. Hirosky[192], M. Jose[192], A. Ledovskoy[192], C. Mantilla[192], C. Neu[192], C. Ramón Álvarez[192], S. Bhattacharya[193], P.E. Karchin[193], A. Aravind[194], S. Banerjee[194], K. Black[194], T. Bose[194], E. Chavez[194], S. Dasu[194], P. Everaerts[194], C. Galloni[194], H. He[194], M. Herndon[194], A. Herve[194], C.K. Koraka[194], S. Lomte[194], R. Loveless[194], A. Mallampalli[194], A. Mohammadi[194], S. Mondal[194], T. Nelson[194], G. Parida[194], D. Pinna[194], L. Pétré[194], A. Savin[194], V. Shang[194], V. Sharma[194], W.H. Smith[194], D. Teague[194], H.F. Tsoi[194], W. Vetens[194], A. Warden[194], S. Afanasiev[195], V. Alexakhin[195], Yu. Andreev[195], T. Aushev[195], D. Budkouski[195], R. Chistov[195,cr], M. Danilov[195,cr], T. Dimova[195,cr], A. Ershov[195,cr], S. Gninenko[195], I. Gorbunov[195], A. Gribushin[195,cr], A. Kamenev[195], V. Karjavine[195], M. Kirsanov[195], V. Klyukhin[195,cr], O. Kodolova[195,ct,cq], V. Korenkov[195], I. Korsakov[195], A. Kozyrev[195,cr], N. Krasnikov[195], A. Lanev[195], A. Malakhov[195], V. Matveev[195,cr], A. Nikitenko[195,cu,cv], V. Palichik[195], V. Perelygin[195], S. Petrushanko[195,cr], S. Polikarpov[195,cr], O. Radchenko[195,cr], M. Savina[195], V. Shalaev[195], S. Shmatov[195], S. Shulha[195], Y. Skovpen[195,cr], K. Slizhevskiy[195], V. Smirnov[195], O. Teryaev[195], I. Tlisova[195,cr], A. Toropin[195], N. Voytishin[195], B.S. Yuldashev[195,cw,†], A. Zarubin[195], I. Zhizhin[195], E. Boos[196], V. Bunichev[196], M. Dubinin[196,cj], L. Dudko[196], K. Ivanov[196], V. Kim[196,cr], V. Murzin[196], V. Oreshkin[196], V. Savrin[196], A. Snigirev[196], D. Sosnov[196]

[1] *Yerevan Physics Institute, Yerevan, Armenia*
[2] *Institut für Hochenergiephysik, Vienna, Austria*
[3] *Universiteit Antwerpen, Antwerpen, Belgium*
[4] *Vrije Universiteit Brussel, Brussel, Belgium*
[5] *Université Libre de Bruxelles, Bruxelles, Belgium*
[6] *Ghent University, Ghent, Belgium*
[7] *Université Catholique de Louvain, Louvain-la-Neuve, Belgium*
[8] *Centro Brasileiro de Pesquisas Fisicas, Rio de Janeiro, Brazil*
[9] *Universidade do Estado do Rio de Janeiro, Rio de Janeiro, Brazil*
[10] *Universidade Estadual Paulista, Universidade Federal do ABC, São Paulo, Brazil*
[11] *Institute for Nuclear Research and Nuclear Energy, Bulgarian Academy of Sciences, Sofia, Bulgaria*
[12] *University of Sofia, Sofia, Bulgaria*
[13] *Instituto De Alta Investigación, Universidad de Tarapacá, Casilla 7 D, Arica, Chile*
[14] *Universidad Tecnica Federico Santa Maria, Valparaiso, Chile*
[15] *Beihang University, Beijing, China*
[16] *Department of Physics, Tsinghua University, Beijing, China*
[17] *Institute of High Energy Physics, Beijing, China*
[18] *State Key Laboratory of Nuclear Physics and Technology, Peking University, Beijing, China*

JHEP03(2026)140

[19] State Key Laboratory of Nuclear Physics and Technology, Institute of Quantum Matter, South China Normal University, Guangzhou, China
[20] Sun Yat-Sen University, Guangzhou, China
[21] University of Science and Technology of China, Hefei, China
[22] Nanjing Normal University, Nanjing, China
[23] Institute of Modern Physics and Key Laboratory of Nuclear Physics and Ion-beam Application (MOE) — Fudan University, Shanghai, China
[24] Zhejiang University, Hangzhou, Zhejiang, China
[25] Universidad de Los Andes, Bogota, Colombia
[26] Universidad de Antioquia, Medellin, Colombia
[27] University of Split, Faculty of Electrical Engineering, Mechanical Engineering and Naval Architecture, Split, Croatia
[28] University of Split, Faculty of Science, Split, Croatia
[29] Institute Rudjer Boskovic, Zagreb, Croatia
[30] University of Cyprus, Nicosia, Cyprus
[31] Charles University, Prague, Czech Republic
[32] Escuela Politecnica Nacional, Quito, Ecuador
[33] Universidad San Francisco de Quito, Quito, Ecuador
[34] Academy of Scientific Research and Technology of the Arab Republic of Egypt, Egyptian Network of High Energy Physics, Cairo, Egypt
[35] Center for High Energy Physics (CHEP-FU), Fayoum University, El-Fayoum, Egypt
[36] National Institute of Chemical Physics and Biophysics, Tallinn, Estonia
[37] Department of Physics, University of Helsinki, Helsinki, Finland
[38] Helsinki Institute of Physics, Helsinki, Finland
[39] Lappeenranta-Lahti University of Technology, Lappeenranta, Finland
[40] IRFU, CEA, Université Paris-Saclay, Gif-sur-Yvette, France
[41] Laboratoire Leprince-Ringuet, CNRS/IN2P3, Ecole Polytechnique, Institut Polytechnique de Paris, Palaiseau, France
[42] Université de Strasbourg, CNRS, IPHC UMR 7178, Strasbourg, France
[43] Centre de Calcul de l'Institut National de Physique Nucleaire et de Physique des Particules, CNRS/IN2P3, Villeurbanne, France
[44] Institut de Physique des 2 Infinis de Lyon (IP2I), Villeurbanne, France
[45] Georgian Technical University, Tbilisi, Georgia
[46] RWTH Aachen University, I. Physikalisches Institut, Aachen, Germany
[47] RWTH Aachen University, III. Physikalisches Institut A, Aachen, Germany
[48] RWTH Aachen University, III. Physikalisches Institut B, Aachen, Germany
[49] Deutsches Elektronen-Synchrotron, Hamburg, Germany
[50] University of Hamburg, Hamburg, Germany
[51] Karlsruher Institut fuer Technologie, Karlsruhe, Germany
[52] Institute of Nuclear and Particle Physics (INPP), NCSR Demokritos, Aghia Paraskevi, Greece
[53] National and Kapodistrian University of Athens, Athens, Greece
[54] National Technical University of Athens, Athens, Greece
[55] University of Ioánnina, Ioánnina, Greece
[56] HUN-REN Wigner Research Centre for Physics, Budapest, Hungary
[57] MTA-ELTE Lendület CMS Particle and Nuclear Physics Group, Eötvös Loránd University, Budapest, Hungary
[58] Faculty of Informatics, University of Debrecen, Debrecen, Hungary
[59] HUN-REN ATOMKI — Institute of Nuclear Research, Debrecen, Hungary
[60] Karoly Robert Campus, MATE Institute of Technology, Gyongyos, Hungary
[61] Panjab University, Chandigarh, India
[62] University of Delhi, Delhi, India
[63] University of Hyderabad, Hyderabad, India
[64] Indian Institute of Technology Kanpur, Kanpur, India

JHEP03(2026)140

[65] *Saha Institute of Nuclear Physics, HBNI, Kolkata, India*
[66] *Indian Institute of Technology Madras, Madras, India*
[67] *IISER Mohali, India, Mohali, India*
[68] *Tata Institute of Fundamental Research-A, Mumbai, India*
[69] *Tata Institute of Fundamental Research-B, Mumbai, India*
[70] *National Institute of Science Education and Research, An OCC of Homi Bhabha National Institute, Bhubaneswar, Odisha, India*
[71] *Indian Institute of Science Education and Research (IISER), Pune, India*
[72] *Indian Institute of Technology Hyderabad, Telangana, India*
[73] *Isfahan University of Technology, Isfahan, Iran*
[74] *Institute for Research in Fundamental Sciences (IPM), Tehran, Iran*
[75] *University College Dublin, Dublin, Ireland*
[76a] *INFN Sezione di Bari, Bari, Italy*
[76b] *Università di Bari, Bari, Italy*
[76c] *Politecnico di Bari, Bari, Italy*
[77a] *INFN Sezione di Bologna, Bologna, Italy*
[77b] *Università di Bologna, Bologna, Italy*
[78a] *INFN Sezione di Catania, Catania, Italy*
[78b] *Università di Catania, Catania, Italy*
[79a] *INFN Sezione di Firenze, Firenze, Italy*
[79b] *Università di Firenze, Firenze, Italy*
[80] *INFN Laboratori Nazionali di Frascati, Frascati, Italy*
[81a] *INFN Sezione di Genova, Genova, Italy*
[81b] *Università di Genova, Genova, Italy*
[82a] *INFN Sezione di Milano-Bicocca, Milano, Italy*
[82b] *Università di Milano-Bicocca, Milano, Italy*
[83a] *INFN Sezione di Napoli, Napoli, Italy*
[83b] *Università di Napoli 'Federico II', Napoli, Italy*
[83c] *Università della Basilicata, Potenza, Italy*
[83d] *Scuola Superiore Meridionale (SSM), Napoli, Italy*
[84a] *INFN Sezione di Padova, Padova, Italy*
[84b] *Università di Padova, Padova, Italy*
[84c] *Universita degli Studi di Cagliari, Cagliari, Italy*
[85a] *INFN Sezione di Pavia, Pavia, Italy*
[85b] *Università di Pavia, Pavia, Italy*
[86a] *INFN Sezione di Perugia, Perugia, Italy*
[86b] *Università di Perugia, Perugia, Italy*
[87a] *INFN Sezione di Pisa, Pisa, Italy*
[87b] *Università di Pisa, Pisa, Italy*
[87c] *Scuola Normale Superiore di Pisa, Pisa, Italy*
[87d] *Università di Siena, Siena, Italy*
[88a] *INFN Sezione di Roma, Roma, Italy*
[88b] *Sapienza Università di Roma, Roma, Italy*
[89a] *INFN Sezione di Torino, Torino, Italy*
[89b] *Università di Torino, Torino, Italy*
[89c] *Università del Piemonte Orientale, Novara, Italy*
[90a] *INFN Sezione di Trieste, Trieste, Italy*
[90b] *Università di Trieste, Trieste, Italy*
[91] *Kyungpook National University, Daegu, Korea*
[92] *Department of Mathematics and Physics — GWNU, Gangneung, Korea*
[93] *Chonnam National University, Institute for Universe and Elementary Particles, Kwangju, Korea*
[94] *Hanyang University, Seoul, Korea*
[95] *Korea University, Seoul, Korea*

JHEP03(2026)140

[96] Kyung Hee University, Department of Physics, Seoul, Korea
[97] Sejong University, Seoul, Korea
[98] Seoul National University, Seoul, Korea
[99] University of Seoul, Seoul, Korea
[100] Yonsei University, Department of Physics, Seoul, Korea
[101] Sungkyunkwan University, Suwon, Korea
[102] College of Engineering and Technology, American University of the Middle East (AUM), Dasman, Kuwait
[103] Kuwait University — College of Science — Department of Physics, Safat, Kuwait
[104] Riga Technical University, Riga, Latvia
[105] University of Latvia (LU), Riga, Latvia
[106] Vilnius University, Vilnius, Lithuania
[107] National Centre for Particle Physics, Universiti Malaya, Kuala Lumpur, Malaysia
[108] Universidad de Sonora (UNISON), Hermosillo, Mexico
[109] Centro de Investigacion y de Estudios Avanzados del IPN, Mexico City, Mexico
[110] Universidad Iberoamericana, Mexico City, Mexico
[111] Benemerita Universidad Autonoma de Puebla, Puebla, Mexico
[112] University of Montenegro, Podgorica, Montenegro
[113] University of Canterbury, Christchurch, New Zealand
[114] National Centre for Physics, Quaid-I-Azam University, Islamabad, Pakistan
[115] AGH University of Krakow, Krakow, Poland
[116] National Centre for Nuclear Research, Swierk, Poland
[117] Institute of Experimental Physics, Faculty of Physics, University of Warsaw, Warsaw, Poland
[118] Warsaw University of Technology, Warsaw, Poland
[119] Laboratório de Instrumentação e Física Experimental de Partículas, Lisboa, Portugal
[120] Faculty of Physics, University of Belgrade, Belgrade, Serbia
[121] VINCA Institute of Nuclear Sciences, University of Belgrade, Belgrade, Serbia
[122] Centro de Investigaciones Energéticas Medioambientales y Tecnológicas (CIEMAT), Madrid, Spain
[123] Universidad Autónoma de Madrid, Madrid, Spain
[124] Universidad de Oviedo, Instituto Universitario de Ciencias y Tecnologías Espaciales de Asturias (ICTEA), Oviedo, Spain
[125] Instituto de Física de Cantabria (IFCA), CSIC-Universidad de Cantabria, Santander, Spain
[126] University of Colombo, Colombo, Sri Lanka
[127] University of Ruhuna, Department of Physics, Matara, Sri Lanka
[128] CERN, European Organization for Nuclear Research, Geneva, Switzerland
[129] PSI Center for Neutron and Muon Sciences, Villigen, Switzerland
[130] ETH Zurich — Institute for Particle Physics and Astrophysics (IPA), Zurich, Switzerland
[131] Universität Zürich, Zurich, Switzerland
[132] National Central University, Chung-Li, Taiwan
[133] National Taiwan University (NTU), Taipei, Taiwan
[134] High Energy Physics Research Unit, Department of Physics, Faculty of Science, Chulalongkorn University, Bangkok, Thailand
[135] Tunis El Manar University, Tunis, Tunisia
[136] Çukurova University, Physics Department, Science and Art Faculty, Adana, Turkey
[137] Middle East Technical University, Physics Department, Ankara, Turkey
[138] Bogazici University, Istanbul, Turkey
[139] Istanbul Technical University, Istanbul, Turkey
[140] Istanbul University, Istanbul, Turkey
[141] Yildiz Technical University, Istanbul, Turkey
[142] Institute for Scintillation Materials of National Academy of Science of Ukraine, Kharkiv, Ukraine
[143] National Science Centre, Kharkiv Institute of Physics and Technology, Kharkiv, Ukraine
[144] University of Bristol, Bristol, U.K.
[145] Rutherford Appleton Laboratory, Didcot, U.K.
[146] Imperial College, London, U.K.

JHEP03(2026)140

[147] *Brunel University, Uxbridge, U.K.*
[148] *Baylor University, Waco, Texas, U.S.A.*
[149] *Bethel University, St. Paul, Minnesota, U.S.A.*
[150] *Catholic University of America, Washington, DC, U.S.A.*
[151] *The University of Alabama, Tuscaloosa, Alabama, U.S.A.*
[152] *Boston University, Boston, Massachusetts, U.S.A.*
[153] *Brown University, Providence, Rhode Island, U.S.A.*
[154] *University of California, Davis, Davis, California, U.S.A.*
[155] *University of California, Los Angeles, California, U.S.A.*
[156] *University of California, Riverside, Riverside, California, U.S.A.*
[157] *University of California, San Diego, La Jolla, California, U.S.A.*
[158] *University of California, Santa Barbara — Department of Physics, Santa Barbara, California, U.S.A.*
[159] *California Institute of Technology, Pasadena, California, U.S.A.*
[160] *Carnegie Mellon University, Pittsburgh, Pennsylvania, U.S.A.*
[161] *University of Colorado Boulder, Boulder, Colorado, U.S.A.*
[162] *Cornell University, Ithaca, New York, U.S.A.*
[163] *Fermi National Accelerator Laboratory, Batavia, Illinois, U.S.A.*
[164] *University of Florida, Gainesville, Florida, U.S.A.*
[165] *Florida State University, Tallahassee, Florida, U.S.A.*
[166] *Florida Institute of Technology, Melbourne, Florida, U.S.A.*
[167] *University of Illinois Chicago, Chicago, Illinois, U.S.A.*
[168] *The University of Iowa, Iowa City, Iowa, U.S.A.*
[169] *Johns Hopkins University, Baltimore, Maryland, U.S.A.*
[170] *The University of Kansas, Lawrence, Kansas, U.S.A.*
[171] *Kansas State University, Manhattan, Kansas, U.S.A.*
[172] *University of Maryland, College Park, Maryland, U.S.A.*
[173] *Massachusetts Institute of Technology, Cambridge, Massachusetts, U.S.A.*
[174] *University of Minnesota, Minneapolis, Minnesota, U.S.A.*
[175] *University of Nebraska-Lincoln, Lincoln, Nebraska, U.S.A.*
[176] *State University of New York at Buffalo, Buffalo, New York, U.S.A.*
[177] *Northeastern University, Boston, Massachusetts, U.S.A.*
[178] *Northwestern University, Evanston, Illinois, U.S.A.*
[179] *University of Notre Dame, Notre Dame, Indiana, U.S.A.*
[180] *The Ohio State University, Columbus, Ohio, U.S.A.*
[181] *Princeton University, Princeton, New Jersey, U.S.A.*
[182] *University of Puerto Rico, Mayaguez, Puerto Rico, U.S.A.*
[183] *Purdue University, West Lafayette, Indiana, U.S.A.*
[184] *Purdue University Northwest, Hammond, Indiana, U.S.A.*
[185] *Rice University, Houston, Texas, U.S.A.*
[186] *University of Rochester, Rochester, New York, U.S.A.*
[187] *Rutgers, The State University of New Jersey, Piscataway, New Jersey, U.S.A.*
[188] *University of Tennessee, Knoxville, Tennessee, U.S.A.*
[189] *Texas A&M University, College Station, Texas, U.S.A.*
[190] *Texas Tech University, Lubbock, Texas, U.S.A.*
[191] *Vanderbilt University, Nashville, Tennessee, U.S.A.*
[192] *University of Virginia, Charlottesville, Virginia, U.S.A.*
[193] *Wayne State University, Detroit, Michigan, U.S.A.*
[194] *University of Wisconsin — Madison, Madison, Wisconsin, U.S.A.*
[195] *An institute or international laboratory covered by a cooperation agreement with CERN*
[196] *An institute formerly covered by a cooperation agreement with CERN*

[a] *Also at Yerevan State University, Yerevan, Armenia*
[b] *Also at TU Wien, Vienna, Austria*

JHEP03(2026)140

[c] Also at Ghent University, Ghent, Belgium
[d] Also at Universidade do Estado do Rio de Janeiro, Rio de Janeiro, Brazil
[e] Also at FACAMP — Faculdades de Campinas, Sao Paulo, Brazil
[f] Also at Universidade Estadual de Campinas, Campinas, Brazil
[g] Also at Federal University of Rio Grande do Sul, Porto Alegre, Brazil
[h] Also at The University of the State of Amazonas, Manaus, Brazil
[i] Also at University of Chinese Academy of Sciences, Beijing, China
[j] Also at China Center of Advanced Science and Technology, Beijing, China
[k] Also at University of Chinese Academy of Sciences, Beijing, China
[l] Also at School of Physics, Zhengzhou University, Zhengzhou, China
[m] Now at Henan Normal University, Xinxiang, China
[n] Also at University of Shanghai for Science and Technology, Shanghai, China
[o] Now at The University of Iowa, Iowa City, Iowa, U.S.A.
[p] Also at Center for High Energy Physics, Peking University, Beijing, China
[q] Also at Helwan University, Cairo, Egypt
[r] Now at Zewail City of Science and Technology, Zewail, Egypt
[s] Also at British University in Egypt, Cairo, Egypt
[t] Now at Helwan University, Cairo, Egypt
[u] Also at Purdue University, West Lafayette, Indiana, U.S.A.
[v] Also at Université de Haute Alsace, Mulhouse, France
[w] Also at Istinye University, Istanbul, Turkey
[x] Also at Another institute or international laboratory covered by a cooperation agreement with CERN
[y] Also at University of Hamburg, Hamburg, Germany
[z] Also at RWTH Aachen University, III. Physikalisches Institut A, Aachen, Germany
[aa] Also at Bergische University Wuppertal (BUW), Wuppertal, Germany
[ab] Also at Brandenburg University of Technology, Cottbus, Germany
[ac] Also at Forschungszentrum Jülich, Juelich, Germany
[ad] Now at RWTH Aachen University, III. Physikalisches Institut A, Aachen, Germany
[ae] Also at CERN, European Organization for Nuclear Research, Geneva, Switzerland
[af] Also at HUN-REN ATOMKI — Institute of Nuclear Research, Debrecen, Hungary
[ag] Now at Universitatea Babes-Bolyai — Facultatea de Fizica, Cluj-Napoca, Romania
[ah] Also at MTA-ELTE Lendület CMS Particle and Nuclear Physics Group, Eötvös Loránd University, Budapest, Hungary
[ai] Also at HUN-REN Wigner Research Centre for Physics, Budapest, Hungary
[aj] Also at Physics Department, Faculty of Science, Assiut University, Assiut, Egypt
[ak] Also at The University of Kansas, Lawrence, Kansas, U.S.A.
[al] Also at Punjab Agricultural University, Ludhiana, India
[am] Also at University of Hyderabad, Hyderabad, India
[an] Also at Indian Institute of Science (IISc), Bangalore, India
[ao] Also at University of Visva-Bharati, Santiniketan, India
[ap] Also at IIT Bhubaneswar, Bhubaneswar, India
[aq] Also at Institute of Physics, Bhubaneswar, India
[ar] Also at Deutsches Elektronen-Synchrotron, Hamburg, Germany
[as] Also at Isfahan University of Technology, Isfahan, Iran
[at] Also at Sharif University of Technology, Tehran, Iran
[au] Also at Department of Physics, University of Science and Technology of Mazandaran, Behshahr, Iran
[av] Also at Department of Physics, Faculty of Science, Arak University, ARAK, Iran
[aw] Also at Italian National Agency for New Technologies, Energy and Sustainable Economic Development, Bologna, Italy
[ax] Also at Centro Siciliano di Fisica Nucleare e di Struttura Della Materia, Catania, Italy
[ay] Also at James Madison University, Harrisonburg, N/A, U.S.A.
[az] Also at Università degli Studi Guglielmo Marconi, Roma, Italy
[ba] Also at Scuola Superiore Meridionale, Università di Napoli 'Federico II', Napoli, Italy

JHEP03(2026)140

[bb] Also at Fermi National Accelerator Laboratory, Batavia, Illinois, U.S.A.
[bc] Also at Laboratori Nazionali di Legnaro dell'INFN, Legnaro, Italy
[bd] Also at Lulea University of Technology, Lulea, Sweden
[be] Also at Consiglio Nazionale delle Ricerche — Istituto Officina dei Materiali, Perugia, Italy
[bf] Also at UPES — University of Petroleum and Energy Studies, Dehradun, India
[bg] Also at Institut de Physique des 2 Infinis de Lyon (IP2I), Villeurbanne, France
[bh] Also at Department of Applied Physics, Faculty of Science and Technology, Universiti Kebangsaan Malaysia, Bangi, Malaysia
[bi] Also at Trincomalee Campus, Eastern University, Sri Lanka, Nilaveli, Sri Lanka
[bj] Also at Saegis Campus, Nugegoda, Sri Lanka
[bk] Also at National and Kapodistrian University of Athens, Athens, Greece
[bl] Also at Ecole Polytechnique Fédérale Lausanne, Lausanne, Switzerland
[bm] Also at Universität Zürich, Zurich, Switzerland
[bn] Also at Stefan Meyer Institute for Subatomic Physics, Vienna, Austria
[bo] Also at Near East University, Research Center of Experimental Health Science, Mersin, Turkey
[bp] Also at Konya Technical University, Konya, Turkey
[bq] Also at Izmir Bakircay University, Izmir, Turkey
[br] Also at Adiyaman University, Adiyaman, Turkey
[bs] Also at Bozok Universitetesi Rektörlügü, Yozgat, Turkey
[bt] Also at Istanbul Sabahattin Zaim University, Istanbul, Turkey
[bu] Also at Marmara University, Istanbul, Turkey
[bv] Also at Milli Savunma University, Istanbul, Turkey
[bw] Also at Informatics and Information Security Research Center, Gebze/Kocaeli, Turkey
[bx] Also at Kafkas University, Kars, Turkey
[by] Now at Istanbul Okan University, Istanbul, Turkey
[bz] Also at Hacettepe University, Ankara, Turkey
[ca] Also at Erzincan Binali Yildirim University, Erzincan, Turkey
[cb] Also at Istanbul University — Cerrahpasa, Faculty of Engineering, Istanbul, Turkey
[cc] Also at Yildiz Technical University, Istanbul, Turkey
[cd] Also at School of Physics and Astronomy, University of Southampton, Southampton, U.K.
[ce] Also at Monash University, Faculty of Science, Clayton, Australia
[cf] Also at Bethel University, St. Paul, Minnesota, U.S.A.
[cg] Also at Università di Torino, Torino, Italy
[ch] Also at Karamanoğlu Mehmetbey University, Karaman, Turkey
[ci] Also at California Lutheran University;, Thousand Oaks, California, U.S.A.
[cj] Also at California Institute of Technology, Pasadena, California, U.S.A.
[ck] Also at United States Naval Academy, Annapolis, Maryland, U.S.A.
[cl] Also at Bingol University, Bingol, Turkey
[cm] Also at Georgian Technical University, Tbilisi, Georgia
[cn] Also at Sinop University, Sinop, Turkey
[co] Also at Erciyes University, Kayseri, Turkey
[cp] Also at Horia Hulubei National Institute of Physics and Nuclear Engineering (IFIN-HH), Bucharest, Romania
[cq] Now at Another institute formerly covered by a cooperation agreement with CERN
[cr] Also at Another institute formerly covered by a cooperation agreement with CERN
[cs] Also at Hamad Bin Khalifa University (HBKU), Doha, Qatar
[ct] Also at Yerevan Physics Institute, Yerevan, Armenia
[cu] Also at Imperial College, London, U.K.
[cv] Now at Yerevan Physics Institute, Yerevan, Armenia
[cw] Also at Institute of Nuclear Physics of the Uzbekistan Academy of Sciences, Tashkent, Uzbekistan
[†] Deceased

JHEP03(2026)140